MAPPING OF RICE PLANT GROWTH FROM AIRBORNE LINE SCANNER USING ANFIS METHOD

A.HADI SYAFRUDIN

GRADUATE SCHOOL

BOGOR AGRICULTURAL UNIVERSITY

BOGOR

2012

STATEMENT

I, A.Hadi Syafrudin, here by stated that this thesis entitled:

Mapping of Rice Plant Growth from Airborne Line Scanner Using ANFIS Method

Is results of my own work during the period of November 2011 until July 2012 and that it has not been published before. The content of the thesis has been examined by the advising committee and the external examiner.

Bogor, July 2012

A.Hadi Syafrudin
G051080101

ABSTRACT

A.HADI SYAFRUDIN. Mapping of Rice Plant Growth From Airborne Line Scanner Using ANFIS Method. Under the supervision of I WAYAN ASTIKA and ANTONIUS B. WIJANARTO.

A map of rice plant growth stage is important information to support food security. Remote sensing data on agricultural land have been taken using an airborne line scanner with three channels (NIR, Red, and Green). Airborne camera used is an engineering model of LISAT (LAPAN IPB satellite) camera. Adaptive Neuro fuzzy interferences system (ANFIS) has been applied to these data to mapping of rice plant growth stage. Twenty four classification scenarios were generated to obtain the best of accuracy. A classification scenario consists of input combination from the original image or image rationing and four types of fuzzy membership function. There are four rice plant growth stages: 1) new rice planting, 2) vegetative rice, 3) reproductive rice, and 4) ripening rice. Other objects classification are non vegetation / fallow and trees. Best accuracy occurred in scenario having input images rationing (MPRI, NDVSI, and SAVI) with trapezoid fuzzy membership function, which gives kappa value 95.76%. Best prediction class is new rice planting and ripening rice with user's accuracy of more than 99% followed by vegetative rice with user's accuracy of 93.48 %, while worst prediction class is reproductive rice with user's accuracy of 74.38 %.

Keyword: Rice Plant Growth Stage, ANFIS, Airborne line scanner

ABSTRAK

A.HADI SYAFRUDIN. Pemetaan Pertumbuhan Tanaman Padi dengan *Airborne Line Scanner* Menggunakan Metode ANFIS. Di bawah Bimbingan I WAYAN ASTIKA dan ANTONIUS B. WIJANARTO.

Peta tahap pertumbuhan tanaman padi merupakan informasi penting untuk mendukung ketahanan pangan. Data penginderaan jauh telah diambil pada lahan pertanian menggunakan *Airborne line scanner* dengan tiga kanal (NIR, Merah, dan Hijau). Kamera yang digunakan adalah *engineering model* kamera LISAT (Satelit LAPAN IPB). Adaptive Neuro fuzzy interferences system (ANFIS) telah digunakan pada data tersebut untuk memetakan tahap pertumbuhan tanaman padi. Dua puluh empat skenario klasifikasi telah dilakukan dan dibandingkan akurasinya. Skenario Klasifikasi merupakan kombinasi masukan dari gambar asli atau perbandingan gambar dan empat jenis fungsi keanggotaan fuzzy. Ada empat klasifikasi tahap pertumbuhan tanaman yaitu padi baru tanam, padi vegetatif, padi reproduksi, dan padi pematangan. Klasifikasi obyek lain adalah pepohonan dan tanah bera atau tanpa vegetasi. Akurasi terbaik terjadi pada skenario dengan masukan perbandingan gambar (MPRI, NDVSI, dan SAVI) dengan fungsi keanggotaan fuzzy - trapesium, dengan nilai kappa 95,76%. Prediksi kelas terbaik adalah padi baru tanam dan padi pematangan dengan akurasi pengguna lebih dari 99% diikuti oleh padi vegetatif dengan akurasi pengguna 93,48%. Kelas prediksi terburuk adalah padi reproduksi dengan akurasi pengguna 74,38%.

Kata Kunci: Tahap Pertumbuhan Tanaman padi, ANFIS, Airborne line scanner

SUMMARY

A.HADI SYAFRUDIN. Mapping of Rice Plant Growth From Airborne Line Scanner Using ANFIS Method. Under the supervision of I WAYAN ASTIKA and ANTONIUS B. WIJANARTO.

In recent years, the problem of food security becomes important issues in Indonesia. Availability of agricultural data and information is an important factor in the formulation of food security policy from central to local government. One of the important agricultural data is the rice plant growth stage map. Fast and reliable monitoring of rice plant growth stages require advanced technology. Inventory and monitoring of rice plant growth stages with ground base method is often unable to follow the pace of change. One method often used is the remote sensing technology.

Remote sensing data were collect by using sensors mounted on airborne or satellites. One type of sensor mounted on airborne is line scanner camera. LISA is a line scanner camera space application that is planned to be used at LAPAN IPB satellites (LISAT). Before used in satellites, this camera needs to be tested using an airborne to map plant growth stages. The main advantage of line scanner sensors is the generation of high resolution images without merging or stitching of images patches like in matrix imaging. With Remote Sensing method and Geographic Information System, area of rice plant growth stage on agricultural land can be classification and calculated. In other disciplines, ANFIS have been a good classifier for medical image classification.

ANFIS is the implementation of fuzzy inference system to adaptive networks for developing fuzzy rules with suitable membership functions to have required inputs and outputs. Using a given input/output data set, the ANFIS method constructs a fuzzy inference system whose membership function parameters are tuned (adjusted) using gradient descent algorithm and least squares estimation method. This study has applied ANFIS and integrating with remote sensing techniques. Remote sensing data can be from the airborne line scanner that captures the agricultural land. Agricultural land has been classified into

several of rice plant growth stages to provide more valuable information.

The objective of this research is to develop a classification method for rice plant growth stage from airborne line scanner using adaptive Neuro Fuzzy Interference System. The study was conducted from November 2011 to July 2012. The study case is in Purasari Villages – District of Leuwiliang - Bogor Regency.

The data used in this study were data from airborne line scanner, which were in taken on 3 November 2010. The resulting data were three images from Green, Red, and NIR channel. The images were obtained from an altitude of 2500 meters, with an airborne speed of 120 knot, and ground resolution of around 0.5 meters. A field survey was conducted on 9 November 2010. Field data is collected based on visual observation and interviewing some existing farmers. The interviewing is important because some land covers may have changed during delay capture images and field survey (6 days).

This research has been done in several steps. They are image pre-processing, classification using ANFIS method, comparisons, and post-processing. From agriculture land data original band (green, red, & NIR) and 13 image rationing band were generated. The image rationing used were RNDVI, MPRI, NDVI, EVI2, RVI, RGRI, GNDVI, NDRGI, NDVSI, TNDVI, GRVI, OSAVI, and SAVI.

Twenty four classifications scenarios were set to compare the result of accuracy. Classification scenarios consist of input combination from the original image or image rationing and four type of fuzzy membership function. There are four classification of rice plant growth stage; 1) new rice planting, 2) vegetative rice, 3) reproductive rice, and 4) ripening rice. Another object classification is non vegetation / fallow and trees. Comparison between the scenarios results were determined by the kappa value, which is calculated from the error (confusion) matrix. The best scenario is a scenario with the highest kappa value. The best scenario would eventually be used for classification or rice plant growth stage mapping.

Geometric correction produced corrected images with dimensions of 917 x 2334 pixels and a ground spatial distance of about 0.47 meter. In this study, the same parameters have been used in each scenario. The parameters were three

input and three membership functions (low, medium, and high), Epoch number = 1000, Step Size= 0.01, Step Size Decrement Rate = 0.9, and Step Size Increment Rate = 1.1. Number of validating samples is 13,220 and number of training samples is 12,657.

Best accuracy results occurred in scenario 22 with input images rationing (MPRI, NDVSI, and SAVI) with trapezoid fuzzy membership function, with kappa value of 95.76%. Worst accuracy results occurred in scenario 1 with the input of original images (Red, Green, and NIR) and with triangle fuzzy membership function, where kappa value was 30.85%. From table above, best class is paddy new planting and paddy ripening with producer's accuracy of more than 97 % and user's accuracy of more than 99% followed by paddy vegetative with producer's accuracy of 93.98 % and user's accuracy of 97.58 %. The class that predicted worse was paddy reproductive with producer's accuracy of 78.61 % and user's accuracy of 74.38 %.

Using automatic classification, results that are not possible especially for high resolution images are often found. Like object with a small area in the other object and object with strange pattern. For plant growth stage mapping, every segment of paddy field must have one result. The study area has been segmented as many as 1172 pieces, with majority class average of 64.097%. Results of rice plant growth stage were obtained after post processing. The mapping of rice plant growth stage is 3.91 hectares of new rice planting, 6.72 hectares of vegetative rice, 2.13 hectares of reproductive rice, and 7.52 hectares of ripening rice.

MAPPING OF RICE PLANT GROWTH FROM AIRBORNE LINE SCANNER USING ANFIS METHOD

A.HADI SYAFRUDIN

A thesis submitted for the Degree of Master of Science in Information Technology for Natural Resources Management Study Program

GRADUATE SCHOOL
BOGOR AGRICULTURAL UNIVERSITY
BOGOR
2012

Research Title   : Mapping of Rice Plant Growth from Airborne Line Scanner Using ANFIS Method

Name   : A.Hadi Syafrudin

Student ID   : G051080101

Study Program   : Master of Science in Information Technology for Natural Resource Management

Approved by,

Advisory Board

<u>Dr. Ir. I Wayan Astika, M.Si</u>   <u>Dr. Antonius B. Wijanarto</u>

Supervisor   Co-Supervisor

Endorsed by,

Program Coordinator   Dean of the Graduate School

<u>Dr.Ir. Hartrisari Hardjomidjojo, DEA</u>   <u>Dr. Ir. Dahrul Syah, M.Sc.Agr</u>

Date of Examination: Date of Graduation:

July 27st, 2012lo,

ACKNOWLEDGEMENT

Thanks and gratitude to The Almighty God for all blessing me during studying in MIT and finished the thesis. My deep appreciation would like to be expressed to all my family, especially my beloved father and my beloved mother for all their support and prayers. Further, I would like to express my Gratitude and sincere appreciation to the following individuals and organizations that contributed to the success of my studies:

1. Dr. I Wayan Astika and Dr. Antonius B. Wijanarto, my supervisors and my co-supervisor for all inputs, corrections, and their guidance during the writing of this thesis research. Thank you also Dr. M. Buce Saleh as external examiner for his suggestion to improve this thesis.

2. Dr. Hartisari Hardjomidjojo as MIT coordinator, lectures, all MIT Staff especially Ms. Devi, and employers for their helper during studying at MIT.

3. My classmates and MIT students, especially I made Anombawa for their spirit and kind cooperation.

4. The head of Satellite Payload division - LAPAN for any extraordinary encouragement.

5. My team in LAPAN ORARI satellite has given me some time to focus on completing this thesis, especially for Yudi, Yadi, Dedy El Amin and Patria.

6. All parties who are not mention one by one. Thank you for helping.

CURRICULUM VITAE

A.Hadi Syafrudin was born in Bangkalan, East Java, Indonesia on Nopember 23, 1980, child of couple Mochammad Roem and Choiriyah. He took formal education including elementary school, junior high school, and senior high school in Bojonegoro, East Java from 1987 until 1999. He holds a bachelor of engineering degree (S.T) from the Department of electrical engineering, Faculty of industrial technology, Sepuluh Nopember Institute of Technology (ITS), Surabaya in 2005. Since 2006, he has been working as an assistant researcher at Satellite Technology Center – National Institute of Aeronautics and Space (LAPAN), in Bogor, Indonesia

TABLE OF CONTENTS

LIST OF TABLES

LIST OF FIGURES

LIST OF APPENDICES

I. INTRODUCTION

1.1   Background

In recent years, the problem of food security becomes important issues in Indonesia. There are many factors, such as conversion of agricultural land, high population growth rates, and the uncertainty of climate. Availability of agricultural data and information is an important factor in the formulation of food security policy from central to local government. One of the important agricultural data is the rice plant growth stage map.

Fast and reliable information about rice plant growth stages ranging from land preparation until harvesting are important for agricultural policy makers in national food security system. The data can be used as a way to provide accurate information about the prediction of crop production before the harvest time arrives. Fast and reliable monitoring of rice plant growth stages requires advanced technology. Inventory and monitoring of rice plant growth stages with ground base method are often unable to follow the pace of change. One of methods often used is the remote sensing technology.

Remote sensing is the science and art of obtaining information about an object, area, or phenomenon through the analysis of data acquired by a device that is not in contact with the object, area, or phenomenon under investigations (Lillesand dan Keifer, 2000). Recording remote sensing data were done by using sensors mounted on airborne or satellites. Ones type of sensor mounted on airborne is line scanner camera. The main advantage of line scanner sensors is the generation of high resolution images without merging or stitching of images patches like in matrix imaging (Reulke et al., 2004).

LISA is a line scanner camera space application, which is planned to be used at LAPAN IPB satellites (LISAT). Before mounted on satellite, this camera needs to be tested using an airborne. This test is used to view the camera's sensor capabilities and reference when the camera is operated space-wire using satellite carrier.

The images of airborne line scanner can be used for interpretation and classification in some rice plant growth stages. Every rice plant growth stage has its own characteristics, in general like fallow, green in vegetative phase, and yellow in generative/ripening phase. The color in every rice plant growth stage will give information, which can be used for age prediction of plant. With Remote Sensing method and Geographic Information System, area of rice plant growth stage on agricultural land can be classified and calculated. The remote sensing methods can automatically recognize the spectral classes that represent rice plant growth stage. In other disciplines, ANFIS has been a good classifier for medical image classification (Monireh et al., 2012).

ANFIS is the implementation of fuzzy inference system to adaptive networks for developing fuzzy rules with suitable membership functions to have required inputs and outputs. Using a given data set, the ANFIS method constructs a fuzzy inference system whose membership function parameters are tuned (adjusted) using gradient descent algorithm and least squares estimation method.

Since this method was introduced in 1993 (Jang, 1993), ANFIS has been used in various studies. For image processing, ANFIS is widely used in biomedical research and the limited use for Remote Sensing applications. More research is needed to determine the ability of ANFIS methods in remote sensing applications. This study has applied ANFIS and integrated with remote sensing techniques. Remote sensing data can be from the airborne line scanner that captures the agricultural land. Agricultural land has been classified into several rice plant growth stages to provide more valuable information.

1.2 Objectives

The objective of this research is to develop a classification method for rice plant growth stage from airborne line scanner using Adaptive Neuro Fuzzy Interference System.

1.3 Output

The outputs of this research are:
- ANFIS model for rice plant growth stage.
- Map of rice plant growth stage.

II. LITERATURE REVIEW

2.1 Remote Sensing for Rice Plant Growth Stage

2.1.1 Rice Plant Growth Stage Mapping

Remote Sensing data provide timely, accurate, synoptic and objective estimation of crop growing conditions or crop growth for developing yield models and issuing yield forecasts at a range of spatial scales (Dadhwal, 2004). The advantage of remote sensing methods is the ability to provide repeated measures from a field without destructive sampling of the crop, which can provide valuable information for precision agriculture applications (Hatfield et al., 2010).

Remote sensing techniques play important roles in crop identification, acreage and production estimation, disease and stress detection, soil and water resources characterization (Patil et al., 2002). Remote sensing technique is dependant from reflectance response of object. To discriminate different rice plant growth stage, we have to differentiate the signature for each growth stage in a region from representative samples at specific times. However, some crop types have quite similar spectral responses at equivalent growth stages (Yang et al., 2008).

Supervised classification algorithms aim at predicting the class label. Supervised classification is one of the most commonly undertaken analyses of remotely sensed data. The output of a supervised classification is effectively a thematic map that provides a snapshot representation of the spatial distribution of a particular theme of interest such as land cover (Imdad et al., 2010).

In general, a supervised classification algorithm consists of two phases: 1) the learning phase, in which the algorithm identifies a classification scheme based on spectral signatures obtained from "training" sites having known class labels (e.g. land cover types), and 2) the prediction phase, in which the classification scheme is applied to other locations with unknown class membership (Samaniego et al., 2008).

The validation of results from image processing has become an inherent component of mapping projects using remote sensing technology. The validation informs about the quality of the results obtained by using remote sensing images and comparing them to the reference data, assuming that these data are accurate (Congalton and Green, 1999).

2.1.2 Image Rationing

The main advantages of ratio images are that they used to reduce the variable effects of illumination condition, thus suppressing of the expression of topography (Crane, 1971). Band rationing is the very simple and powerful technique in the remote sensing. Basic idea of this technique is to emphasize or exaggerate the anomaly of the target object (Abrams, 1983). Some formula about image rationing is described in Table 2-1.

Table 2-1   Image Ratio Formula

No	Image Ratio	Formula	References
1	Ratio normalized difference veg. Index	$RNDVI = (NIR^2 - R)/(NIR + R^2)$	Gong et al., 2003
2	Modified Photochemical reflectance Index	$MPRI = (G-R)/(G+R)$	Yang et al., 2008
3	Normalized difference vegetation index	$NDVI = (NIR-R)/(NIR+R)$	Rouse et al., 1973
4	2-band Enhanced vegetation index	$EVI2 = 2.5(NIR - red)/(NIR + red + 1)$	Jiang et al. 2007
5	Ratio vegetation index	$RVI = NIR/R$	Jordan, 1969
6	Red green ratio index	$RGRI = R/G$	Yang et al., 2008
7	Green normalized difference vegetation index	$GNDVI = (NIR - G)/(NIR + G)$	Gitelson et al., 1996
8	Normalized difference red green index	$NDRGI = (R - G)/(R + G)$	Yang et al., 2008
9	Normalized difference vegetation structure index	$NDVSI = [NIR - (R+G) \times 0.5] / [NIR + (R+G) \times 0.5]$	Yang et al., 2008
10	Transformed NDVI	$TNDVI = [(NIR-R) /(NIR+R)+1]^{1/2}$	Tucker, 1979
11	Green ratio veg Index	$GRVI = NIR/G$	Yang et al., 2008
12	Optimal soil adjusted vegetation index	$OSAVI = (NIR - R)/(NIR + R + 0.16)$	Rondeaux et al., 1996
13	Soil-Adjusted Vegetation Index	$SAVI = ((NIR-Red)/(NIR+Red+0.5)) \times (1+0.5)$	Huete A.R, 1988

2.1.3 Related Research of Rice Plant Growth Stage

Some studies have been conducted to map rice plant growth stage. The summary of study on rice plant growth stage is described in Table 2-2.
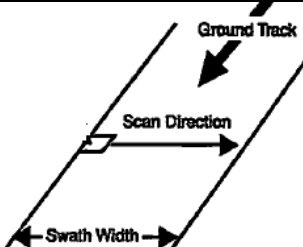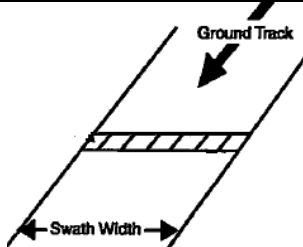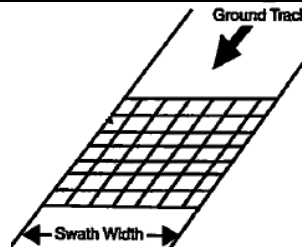
Table 2-2   Summary of Study on Rice Plant Growth Stage

No	Data	Methods	Accuracy	Kappa	Class	Referens
1	LANDSAT	CRUISE - West Java	-	0.91	Fallow, Wet, Vegetative, Generative	Panuju et al., 2008
		CRUISE - East Java	-	0.87		
		QUEST - West Java	-	0.89		
		QUEST - East Java	-	0.87		
2	ALOS AVNIR-2	QUEST	93.90%	-	Fallow, New Planting, Vegetative, Generative	Tjahjono et al., 2009
		CRUISE	89.30%	-		

2.2   Airborne Line Scanner

An airborne line scanner is a camera/sensor, which uses line scanner technique mounted on aircraft. Line scanner technique is one of some scanning technique. Table 2-3 describes the scanning technique utilized in some satellites or Airborne.

Table 2-3   Scanning Technique and Utilization (Wertz et al., 1999).

Scanning technique and utilization		
Whiskbroom Scanner	Line Scanner	Matrix Scanner
Utilized on LANDSAT TM & LANDSAT MSS	Utilized on ALOS, SPOT5 and Quickbird	Utilized on Airborne - Aerial photography , Lapan TubSat

Each scanning technique has advantages and disadvantages. The line scanner technique performance compared with other technique is described in Table 2-4.

Table 2-4   Comparison of Scanning Technique (Wertz et al., 1999)

Technique	Advantages	Disadvantages
Whiskbroom Scanner	High uniformity of the response function over the scene, Relatively simple optics	Short dwell time per pixel, High Bandwidth requirement and time response detector, mechanical scanner required
Line Scanner	Uniform response function in the along direction, No mechanical scanner required, relative long dwell time	High number of pixels per line imager required, relative complex optics
Matrix Scanner	Well defined geometry within the image, long integration time (if motion compensation is performed)	High Number of pixels per matrix imager required, complex optics required covering the full images size, calibration of fixed pattern noise each pixel, High complex scanner required (if motion compensation is performed).

2.2.1 LISA (Line Scanner Space Application)

The LISA II is an engineering model of LAPAN IPB Satellites (LISAT), designed for scanning scientific imaging in space applications. LISA II describes in Figure 2-1.
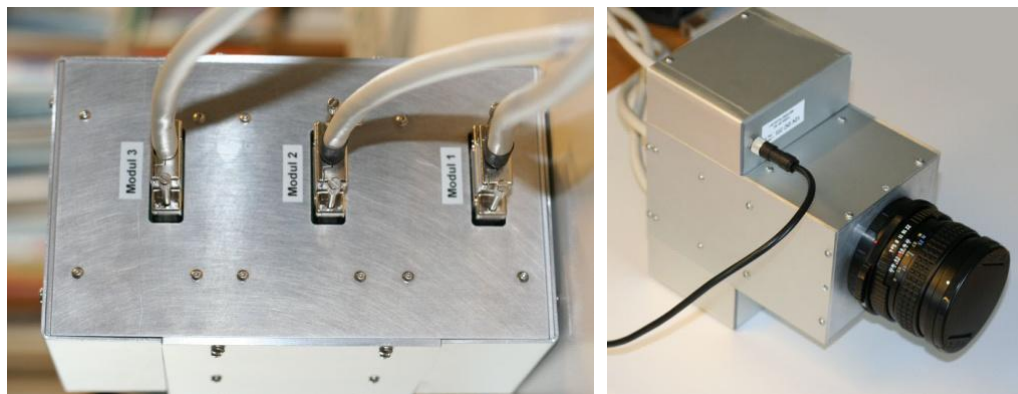
Figure 2-1   Theta Line Scanner Imagers

LISA II use CCD KLI-8023 monochrome and RGB type with customize filter. CCD KLI 8023 is one type of CCD line sensor produced by Eastman Kodak Company - Image Sensor Solutions. This type CCD has two types, first is monochrome and second is Visible Channel (RGB) type. The figure of CCD KLI 8023 (monochrome and RGB) is described in figure 2-2.
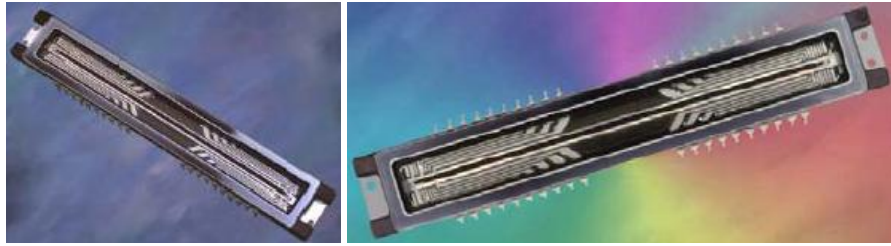
Figure 2-2   KLI-8023 (Monochrome & RGB)

The monochrome CCD has an advantage to modify or customize wavelength, with luminance value measurement by add external filter. Luminance is the total luminous flux incident on a surface, per unit area. It is a measure of the intensity of the incident light, wavelength-weighted by the luminosity function to correlate with human brightness perception. For special purpose, the CCD added with external filter to get spectral response as needed. Schematic of this camera is described in figure 2-3.
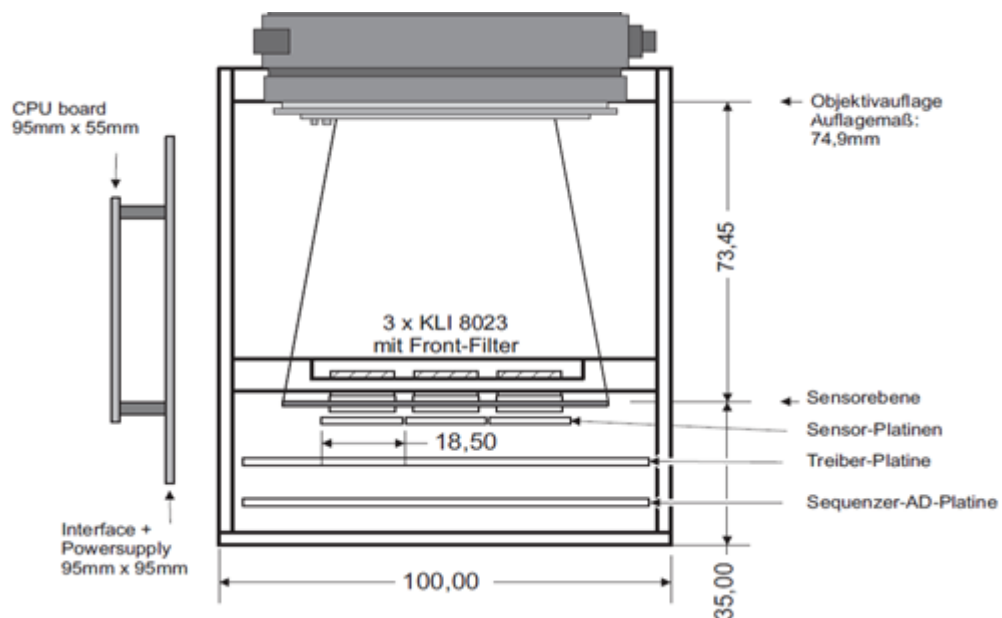
Figure 2-3   LISA II Schematic (THETA Aerospace, 2010)

One quality parameter of CCD sensors is efficiency (input–output gain of a detector system). The efficiency of a sensor for detecting light as a function of wavelength can be presented as a quantum efficiency (QE) curve or a spectral responsivity curve. The spectral responsivity curve of LISA II and comparison with LANDSAT 4, 5, 7 is described in figure 2-4 and detail specification this camera is described in Table 2-5.
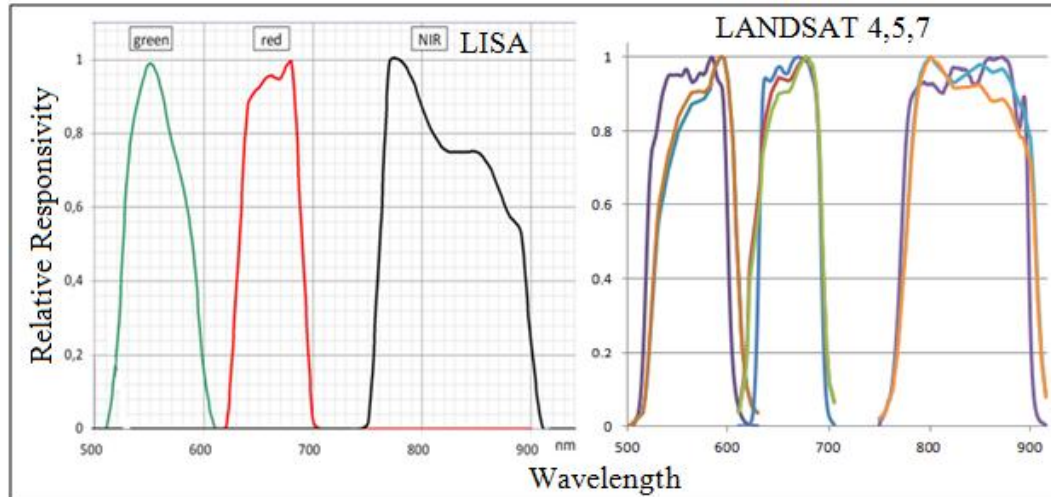
Figure 2-4   Responsivity of LISA Camera & LANDSAT

Table 2-5   Specifications of LISA II (THETA Aerospace, 2010)

Specifications	
Sensor Type	CCD Tri-linear Sensor
Sensor Format	3 x 8002 pixel
Image Size	3 x 72.018mm x 0.009mm, 18.5 mm inter-array-spacing
Responsivity	G (@550nm): 19 V/μJ/cm²
	R (@650nm): 28 V/μJ/cm²
	NIR (@850nm): 18 V/μJ/cm²
Spectrum Bands	G: 520nm – 600nm
	R :630nm – 680nm
	NIR: 780nm – 900nm
Pixel Size	9μm x 9μm
Dark Current	@ 15° C 0.002pA/pixel
Digitalization	16-bit
Max. pixel freq	6 MHz, selectable
Frame Rate	500Hz, adjustable
Integration Time:	10μs to 1/frame rate, adjustable
Lens	Pentax-67, 45 mm/F5.6
Gain	6 x, adjustable
GSD/Swath Width	0.5 meter /4001m (@ Altitude:2500 m)
Co-Registration with NIR channel	R (@2500m/120 Knot): 16.65 ms , 1027.8 m
	Green(@2500m/120 Knot): 33.69 ms, 2055,6 m

LISA II does not used beam splitter and inter spacing array 18.5 mm. It means that at the same time, each sensor channel captures different place. To solve the problem need co-registration process. Image size and co-registration process is described in Figure 2-5.
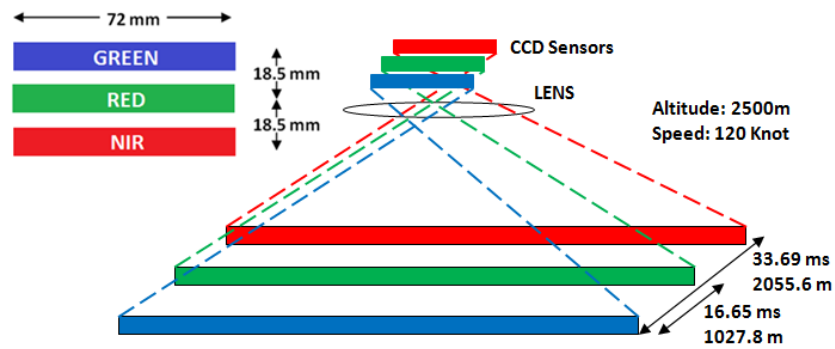
Figure 2-5   Image Size and Co-Registration (THETA Aerospace, 2010)

Co-registration process is technique to delay starting another channel so each channel captures same places. For altitude 2500m and speed 120 knot, the red channel will start capturing after 16.65 ms or 1027.8 m after NIR channel start. For good result, Line scanning required high stabilize attitude (pitch, yaw, raw), constant altitude, and constant speed during scanning process.

2.2.2   Related Research of Airborne Remote Sensing

There are some studies on classification using airborne remote sensing data (Table 2-6). With variety of object classed sensor, and classification methods.

Table 2-6   Related Research of Airborne Remote Sensing

No	Object	Data	Method	Result	Ref
1	Coastal Habitats	ITRES Compact Airborne Spectrographic Imager	MLP Neural Network	Overal Accuracy (OA): 0.826	Brown, 2004
2	Vegetation Mapping	AISA Eagle sensor	Optimized Spectral Angle Mapper	overall weighted accuracy: 67%	Bertels, et al., 2005
3	oil contaminated wetland	Airborne Imaging Spectro Radiometer Applications (AISA)	maximum likelihood	OA:87.6%, kappa: 0.8464	Salem et al., 2005
4	Vegetation Class	Digital Airborne Imagery System	Nearest Neighbor	OA: 58%	Yu et al., 2006
5	separating giant salvinia	Airborne multispectral digital videography	minimum spectral distance	OA: 82.0% kappa: 0.7318	Fletcher et al., 2010

As seen in Table 2-6, airborne remote sensing technologies play important role in measuring and monitoring our natural resources.

2.3 ANFIS

ANFIS, fuzzy inference systems using adaptive network, was proposed to avoid the weak points of fuzzy logic. In this section, classes of adaptive networks, which are functionally equivalent to fuzzy inference systems, were proposed (Jang, 1993).

2.3.1 Fuzzy Interferences System (FIS)

The fuzzy inference system is a popular computing framework based on the concepts of fuzzy set theory, fuzzy if-then rules, and fuzzy reasoning. The fuzzy inferences system is described in Figure 2-6.
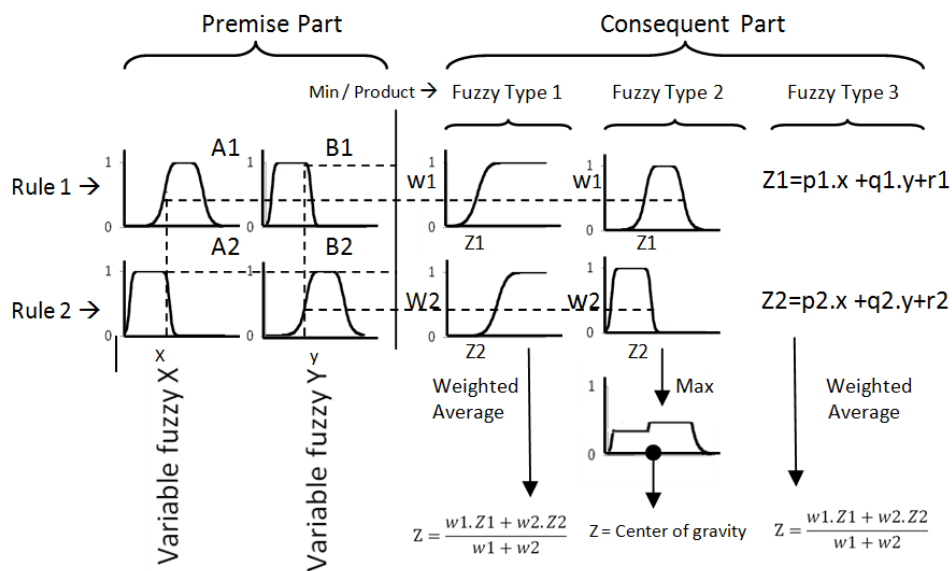
Figure 2-6   Fuzzy Interference System (Jang, 1993).

2.3.2 ANFIS Structure
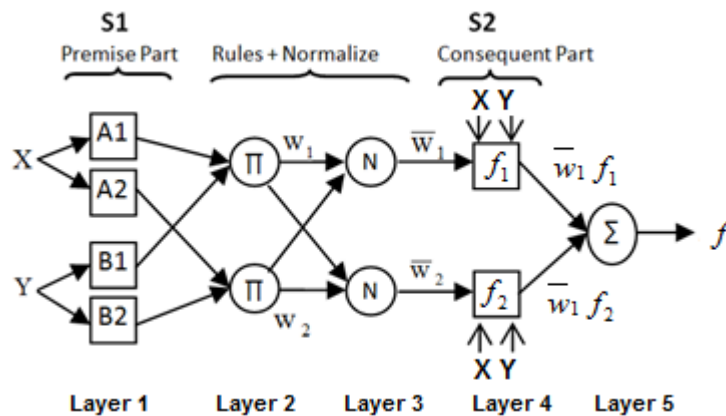
Figure 2.7   ANFIS with 2 Rules (Jang, 1993)

For complex calculation, number of each node is described in Table 2.7. The number of fuzzy input variable is expressed as "M" and number of fuzzy membership function expressed as "P".

Table 2-7   Node and Parameter ANFIS (Jang, 1993)

Layer	Layer Type	Number of Nodes	Number of Parameter
1	Membership function (Tri/Traph/Gauss/GBell)	P.M	(3/4/2/3).P.M = Premise Parameter
2	Rules	P^M	0
3	Normalize	P^M	0
4	Linier Function	P^M	(M+1). P^M = Consequent Parameter
5	SUM	1	0

- Layer 1, the output of each node is:

$$O_{1,i} = \mu_{A_i}(x) \qquad for\ i = 1,2$$

$$O_{1,i} = \mu_{B_{i-2}}(y) \qquad for\ i = 3,4$$

- Layer 2, every node in this layer is fixed. This is where the t-norm is used to 'AND' the membership grades - for example the product:

$$O_{2,i} = w_i = \mu_{A_i}(x).\mu_{B_i}(y), \quad i = 1,2$$

- Layer 3, contains fixed nodes, which calculate the ratio of the firing strengths of the rules:

$$O_{3,i} = \overline{w_i} = \frac{w_i}{w_1 + w_2}$$

- Layers 4, the nodes in this layer are adaptive and perform the consequent of the rules:

$$O_{4,i} = \overline{w_i} f_i = \overline{w_i}(p_i x + q_i y + r_i)$$

The parameters in this layer (p_i, q_i, r_i) are to be determined and are referred to as the consequent parameters.

- Layer 5, there is a single node here that computes the overall output:

$$O_{5,i} = \sum_i \overline{w_i} f_i = \frac{\sum_i w_i f_i}{\sum_i w_i}$$

2.3.3 ANFIS Learning

ANFIS have forward and backward passes of the hybrid learning algorithm. Table 2-8 summarizes the activities in each pass.

Table 2-8   ANFIS Learning (Jang, 1993)

	Forward pass	**Backward pass**
Premise parameters	Fixed	Gradient descent
Consequent parameters	Least-squares estimator	Fixed
Signals	Node outputs	Error signals

a) Forward Pass Learning

In the forward pass of the hybrid learning algorithm node outputs go forward until layer 4 and the consequent parameters are identified by the least-squares method. When the values of the premise parameters are fixed the overall output can be expressed as a linear combination of the consequent parameters.

$$f = \overline{w}_1\, f_1 + \overline{w}_1\, f_2$$

$$f = (\overline{w}_1\, x)p_1 + (\overline{w}_1\, y)q_1 + (\overline{w}_1)r_1 + (\overline{w}_2\, x)p_2 + (\overline{w}_2\, y)q_2 + (\overline{w}_1)r_2$$

Where, {p1, q1, r1, p2, q2, r2} are consequent parameters in layer 4. For given fix values of premise parameters, using K training data, it can transform the above equation into B=AX, where X contains the elements of consequent parameters. This is solved by: $(A^TA)^{-1}A^T\, B=X^*$ where $(A^TA)^{-1}A^T$ is the pseudo-inverse of A (if A^TA is nonsingular). The LSE minimizes the error $\|AX\text{-}B\|^2$ by approximating X with X*

b) Backward Pass Learning

In the backward pass, the error signals propagate backward and the premise parameters are updated by gradient descent. Assuming the given training data set has P entries, we can define the error measure for p^{th} ($1 \le p \le P$) entry of training data entry as the sum of squared errors:

$$E_p = \sum_{m=1}^{\#(L)} (T_{m,p} - O_{m,p}^L)^2$$

where:

$T_{m,p}$ = m^{th} component of pth target output vector;

O^L_{mp} = m^{th} component of actual output vector ; and

#(L)   = Number nodes in Layer L.

Hence the overall error measure can be expressed as

$$E = \sum_{p=1}^{P} E_p .$$

For each parameter α_i the update formua is:

$$\Delta\alpha_i = -\eta \frac{\partial^+ E}{\partial\alpha_i}$$

where:

$$\eta = \frac{k}{\sqrt{\sum_i (\frac{\partial E}{\partial\alpha_i})^2}}$$ Is the learning rate;

k   is the step size; and

$\frac{\partial^+ E}{\partial\alpha_i}$ is the ordered derivative.

2.3.4 Related Research of ANFIS Prediction

There are some studies on classification or prediction using ANFIS algorithms (Table 2-9).

Table 2-9   Related Research of ANFIS

No	Object	Data	Performance	References
1	Oil Spill	MODIS-Terra, MODIS Aqua,Envisat-ASAR	under the ROC curve of 80%	Corucci et al., 2010
2	Crop Yield Prediction	Statistical winter wheat data for 1999-2004	Overall Accuracy: 74%	Stathakis et al., 2006
3	Burnt area by wildfires	MODIS-Terra, NOAA, Meteosat8	Prod Accuracy : 76% User Accuracy : 86%	Calado et al., 2006

As shown in table 2-9, the smallest error of ANFIS training often depends on the number and type membership function. One research of comparison number and type of membership function on three cases is described in Table 2-10.

Table 2-10   Membership Function Comparison (Efendigil et al., 2009).

Number of MF	Type of MF	Study Cases					
		Retailer 1		Retailer 2		Retailer 3	
		MSE	Best	MSE	Best	MSE	Best
2	triMF	0.767	gauss MF	0.315	gbell MF	1.565	trap MF
	trapMF	0.873		0.303		1.241	
	gbellMF	0.676		0.248		1.332	
	gaussMF	0.669		0.253		1.334	
3	triMF	0.424	gbell MF	0.199	gauss MF	1.042	trap MF
	trapMF	0.423		0.212		0.971	
	gbellMF	0.285		0.195		1.394	
	gaussMF	0.286		0.165		0.986	
4	triMF	0.261	trap MF	0.157	trap MF	0.952	tri MF
	trapMF	0.074		0.105		1.018	
	gbellMF	0.232		0.312		0.968	
	gaussMF	0.26		0.15		0.982	
Best MF (Number / type)		0.074	4 MF / trapMF	0.105	4 MF / trapMF	0.952	4 MF / triMF

2.3   Classification Accuracy

Error matrix is a square array of numbers set out in rows and columns that expresses the number of sample units assigned to a particular category in one classification relative to the number of sample units assigned to a particular category in another classification. Mathematical example of an error matrix is described in table 2-11.

Table 2-11   Error Matrixes (Congalton and Green 1999).

		j = Columns (References)			Row Total
		1	2	k	n_{i+}
i=Rows (Classification)	1	n_{11}	n_{12}	n_{1k}	n_{1+}
	2	n_{21}	n_{22}	n_{2k}	n_{2+}
	k	n_{k1}	n_{k2}	n_{kk}	n_{k+}
Column Total	n_{+j}	n_{+1}	n_{+2}	n_{+k}	n

Overall accuracy, producer accuracy, user accuracy and kappa coefficient between remotely sensed classification and the reference data derived from error matrix can then be computed as follows (Congalton and Green, 1999).

$$Overall\_Accuracy = \frac{\sum_{i=1}^{k} n_{ii}}{n}$$

$$Producer's\_Accuracy(j) = \frac{n_{jj}}{n_{+j}}$$

$$User's\_Accuracy(i) = \frac{n_{ii}}{n_{i+}}$$

$$Kappa\_Coefficien\,t = \frac{n\sum_{i=1}^{k} n_{ii} - \sum_{i=1}^{k} n_{i+}n_{+i}}{n^2 - \sum_{i=1}^{k} n_{i+}n_{+i}}$$

where:

$\sum_{i=1}^{k} n_{ii}$: The sum of major diagonal (the correctly classified sample unit);

n : the total number of sample units;

n_{jj} : the total number of correct sample unit in "class x";

n_{+j} : total number of "class x" as indicated by the reference data;

n_{ii} : the total number of correct pixels in the "class x"; and

n_{i+} : the total number of pixels classified as "class x".

III. METHODOLOGY

3.1 Time and Location

The study was conducted from November 2011 to July 2012 . The study case was in Purasari Villages – District of Leuwiliang - Bogor Regency. The location of study area can be seen in Figure 3. From this figure flight path of airborne line scanner flight in regency map, image location in district map, image location (red box) and area of interest (green box) in village map are displayed.
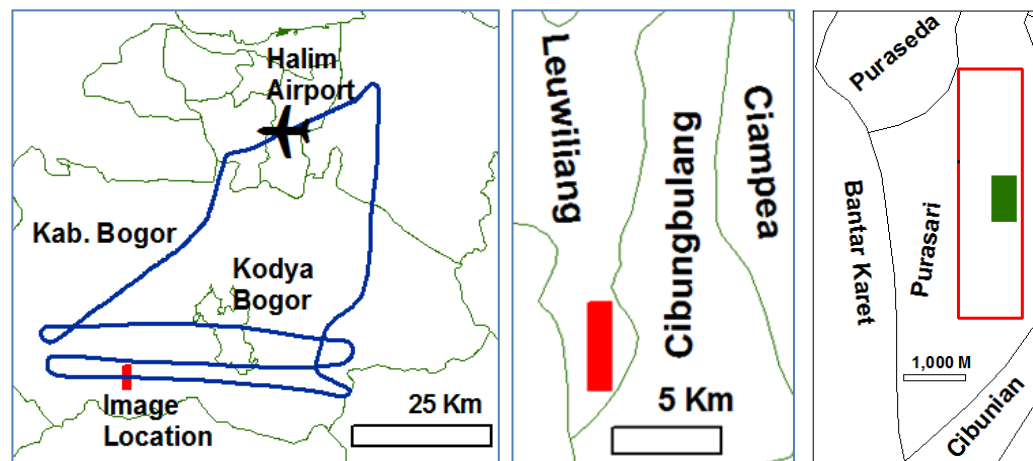
Figure 3-1   Study Area

3.2 Data Collection and Field Survey

3.2.1 Remote Sensing Data

The data used in this study were data from airborne line scanner taken on 3 November 2010. The data resulted into three images from Green, Red, and NIR channels. Data obtained from an altitude of approximately 2500 meters above mean sea level, with an average airborne speed of 120 knots, and ground resolution produced around 0.5 meter.

3.2.2 Field Survey Data

A field survey was conducted on 9 November 2010. Field data is collected based on visual observation and interview existing farmers. Interview method is important because some land cover change during delay capture images and field

survey (6 days). This field observation was intended to label the names of classes. Tools used for the survey are GPS, manual compass, and an 8 megapixel camera. GPS type used was GPS-60 with accuracy $\pm$ 15 meters. Thirty two points of GPS is taken together with fourth photos in each direction (North, South, West, and East). With GPS positioning error of 15 meters, a loop buffer with a radius of 15 meters was made. By utilizing photos with four directions the position was corrected using visual interpretation. Where taking pictures has always been on the field boundary and never was in the center of fields. Example of field survey data is described in Figure 3-2.
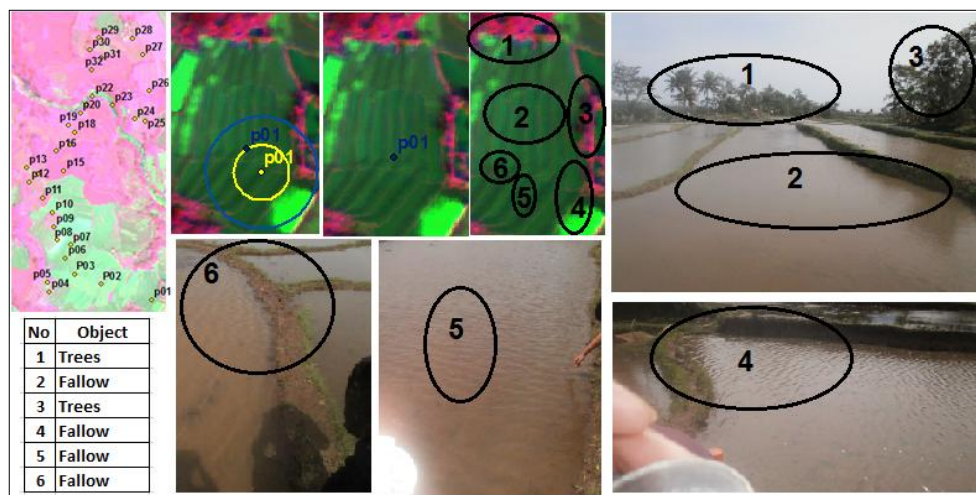
Figure 3-2   Example of Field Survey

3.2.3 Supporting Data

For geometric correction, airborne line scanner data need supporting data. The resulting images on the flight test had a high resolution and are in agricultural areas, this is not possible to perform direct geo-referencing with road map - RBI or use the GPS data that has an error rate of more than one pixel. The geometry corrections must be conducted with raster that have been corrected with RBI map. Supporting data, which used in this research are shown in Table 3-1.

Table 3-1   Supporting Data

No	Data	Producer	Year
1	Road - RBI	Bakosurtanal	2000
2	Contour 25 m - RBI	Bakosurtanal	2000
3	Raster High Resolution	Google Earth Pro	Captured 2010

3.3 Software Required

This research needs some application software to process and training data. The application software's for the overall processes in this study are described in Table 3-2.

Table 3-2   Software Required

Software	Function
ArcGis 9.2	Georeferencing, Map Layout, Image - Ascii converter, Create Training & Test data
PCI Geomatics	Orthorectifity Airborne Result
Visual Basic 6	ASCII - Table converter, Accuracy Calculation, Majority Filter segment.
Matlab 2008	Application Fuzzy type 3, ANFIS Training
MS Excel 2007	Manual Calculation
MS Word 2007	Reporting

3.4 Research Step

This research was done in some steps. They are image pre-processing, classification using ANFIS method, comparisons, and post-processing. The general methodology describes in figure 3-3.
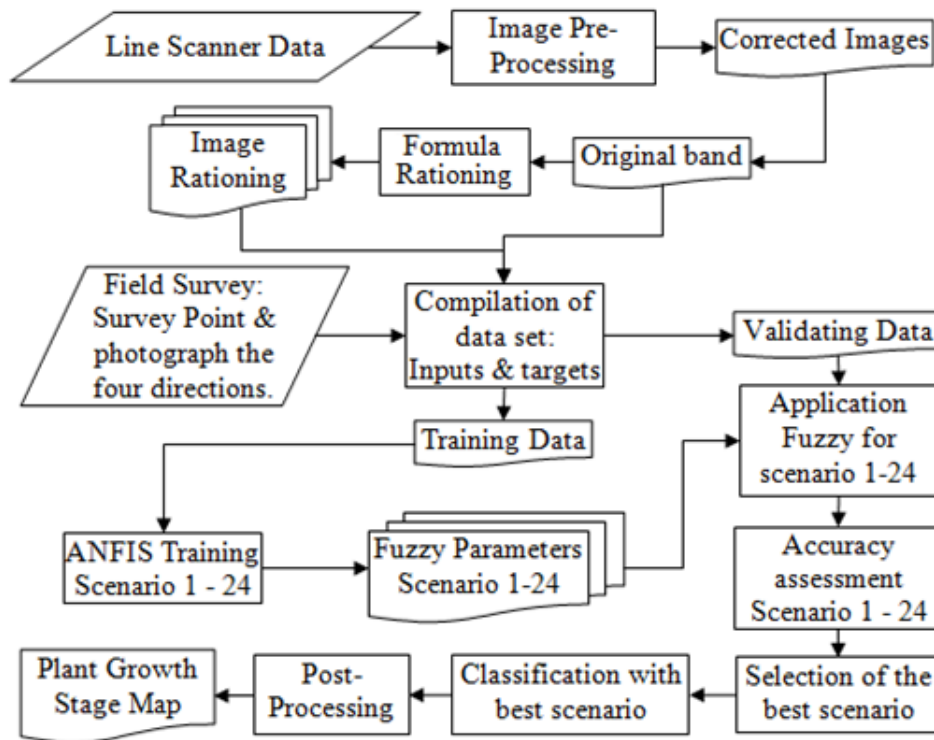
Figure 3-3   Flowchart of General Methodology

3.4.1 Image Pre-Processing

Image pre-processing was done before image classification. There are two standard pre-processing, radiometric correction and geometric correction. Radiometric error due to sun angle and topography will be reduced by using image rationing. Atmospheric correction has not been used in this study, but it is expected will have no error contribution due to the low flying height.

For airborne line scanner, geometric correction was used for co-registration and geo-referencing. Co-registration was done for geometric correction of the green and red channels with reference to the NIR channel. NIR channel was chosen because the channel is the first time to take the pictures and the position closest to the center of gravity of the airborne. Because it is closest to the center of gravity, it has the smallest geometric error due to variations in airborne attitude. This camera is designed for satellite, and does not have stabilization mechanism. Result of this co-registration process was a composite image.

This composite image was geometric corrected using a map reference that has spatial data and DEM from contour RBI interpolation, with Ortho-rectification methods. All data used in this study were registered to RBI map.

3.4.2 Classification Using ANFIS Method

This study classified agricultural land covers using ANFIS method. From agriculture land, data can generate to original band (greed, red, & NIR) and image rationing band as described in Table 2-1. Training and validation data were made based on survey data. Refer to this survey; the classification was done in to 6 classes. These classes were fallow/non vegetation, new rice Planting, vegetative rice, reproductive rice, ripening rice, and trees.

The training data were the target for ANFIS training. To obtain the best classification, six groups of scenarios were tested. Each group consists of four types of membership functions. Each scenario in ANFIS training produced FIS type-3 parameter. These parameters were used in the FIS type-3 with input test data. Results of training and validation process were checked for accuracy. Detail scenario for ANFIS training is described in Table 3-3.

Table 3-3   Scenario ANFIS Training

No	X	Y	Z	MF	No	X	Y	Z	MF	No	X	Y	Z	MF
1	Red	Green	NIR	A	9	NDVI	GNDVI	NDGRI	A	17	RNDVI	MPRI	TNDVI	A
2	Red	Green	NIR	B	10	NDVI	GNDVI	NDGRI	B	18	RNDVI	MPRI	TNDVI	B
3	Red	Green	NIR	C	11	NDVI	GNDVI	NDGRI	C	19	RNDVI	MPRI	TNDVI	C
4	Red	Green	NIR	D	12	NDVI	GNDVI	NDGRI	D	20	RNDVI	MPRI	TNDVI	D
5	RVI	RGRI	GRVI	A	13	EVI 2	OSAVI	SAVI	A	21	MPRI	NDVSI	SAVI	A
6	RVI	RGRI	GRVI	B	14	EVI 2	OSAVI	SAVI	B	22	MPRI	NDVSI	SAVI	B
7	RVI	RGRI	GRVI	C	15	EVI 2	OSAVI	SAVI	C	23	MPRI	NDVSI	SAVI	C
8	RVI	RGRI	GRVI	D	16	EVI 2	OSAVI	SAVI	D	24	MPRI	NDVSI	SAVI	D

* N0: Scenario, X: Variable Fuzzy 1, Y: Variable Fuzzy 2, Z: Variable Fuzzy 3, MF: Type of Fuzzy Membersip Function, A:Triangle, B:Trapezoid, C: Gaussian, D:General Bell

3.4.3 Comparison

Validation step was conducted to test the relationship between prediction and target output. The Error (confusion) matrix was used in this study to find the overall accuracy, producer's accuracy, user's accuracy, and kappa statistic for classification result. The sample data that were used for training process were not used in this accuracy assessment. Comparison between the scenarios results was determined by the kappa value, calculated from the error (confusion) matrix. The best scenario has been a scenario with the highest kappa value. The best scenario would eventually be used for classification or rice plant growth stage mapping.

3.4.4 Image Post-Processing

On the result of automatic classification, often found results that are not possible especially for high resolution images. Like object with a small area in the other object and object with strange pattern. For plant growth stage mapping, every segment of paddy field must be have one result. At post processing, the following procedures were applied:

1. Creating line boundary;
2. Converting line to polygon;
3. Calculating number of pixel each class in one polygon; and
4. Computing the majority class, this will be the result of the polygon.

IV. RESULTS AND DISCUSSIONS

4.1   Image Pre-Processing

The main advantage of line scanner sensors is the ability to generate high resolution images without merging or stitching of images patches like in matrix imaging (Reulke et al., 2004). Line scanner camera has other advantages and disadvantages compared to other scanner types. These can be seen in Table 2-4. The main difference between matrix scanner and line scanner is on the time used for recording each row in images frame.

On matrix scanner, each line in the images is recorded at the same time. In line scanner, each line in the images is recorded at the different time. One thing that causes geometric error in the images is the camera stability. In matrix scanner, geometric errors pattern will occur in each images frame. In line scanner, geometric errors pattern will occur in each line of images frame. This fact cause the line scanner needs more ground control point (GCP) than matrix scanner for off nadir position.

With less stable airborne attitudes and varying altitude of objects on earth, more than 200 control points for co-registration process were used. Number of control points used to obtain the least geometric error and good visualization. Detailed results of geometric correction are described in Table 4-1.

Table 4-1   Result of Geometric Correction

No	Process	References	Method	GCP	RMSE
1	Registration Images References	Road - RBI	Spline	29	0.01
2	Co-Registration Red Channel	NIR Channel	3rd Polynomial	219	0.29
3	Co-Registration Green Channel	NIR Channel	3rd Polynomial	202	0.35
4	Orthorectifity Composite Images	Images References corrected + DEM RBI	Rational Function	79	0.47

From Table 4-1, all geometric correction error has a value of less than 0.5 pixel. In this geometric correction RMS error is below one. So it will provide the

high quality geo-referenced image (Santhosh et al., 2011). Geometric correction produces corrected images with dimensions 917 x 2334 pixel and ground spatial distance 0.47 meter. A corrected image is shown in Appendix 1.

4.2   Field Survey

Congalton and Green (1999) stated that actual ground visitation may be the only reliable method of data collection. A subset of data should be collected on the ground and compared with the image data to verify the reliability of the image reference data. In this study the reference data were taken by visual interpretations that were then compared with field survey data.

Agricultural land was classified into six classes: Fallow/Non vegetation, new rice planting, vegetative rice, reproductive rice, ripening rice, and trees. These classes were the majority of objects found in the study area. These classes were chosen because of the limited number of sensors and analysis based solely on the color of objects. The comparison of class in the images and class in the photo survey is described in Figures 4-1 to 4-6.

a) Man-Made Fish Ponds

b) Fallow Rice Fields with Water Cover

c) Shallow River and Rocks
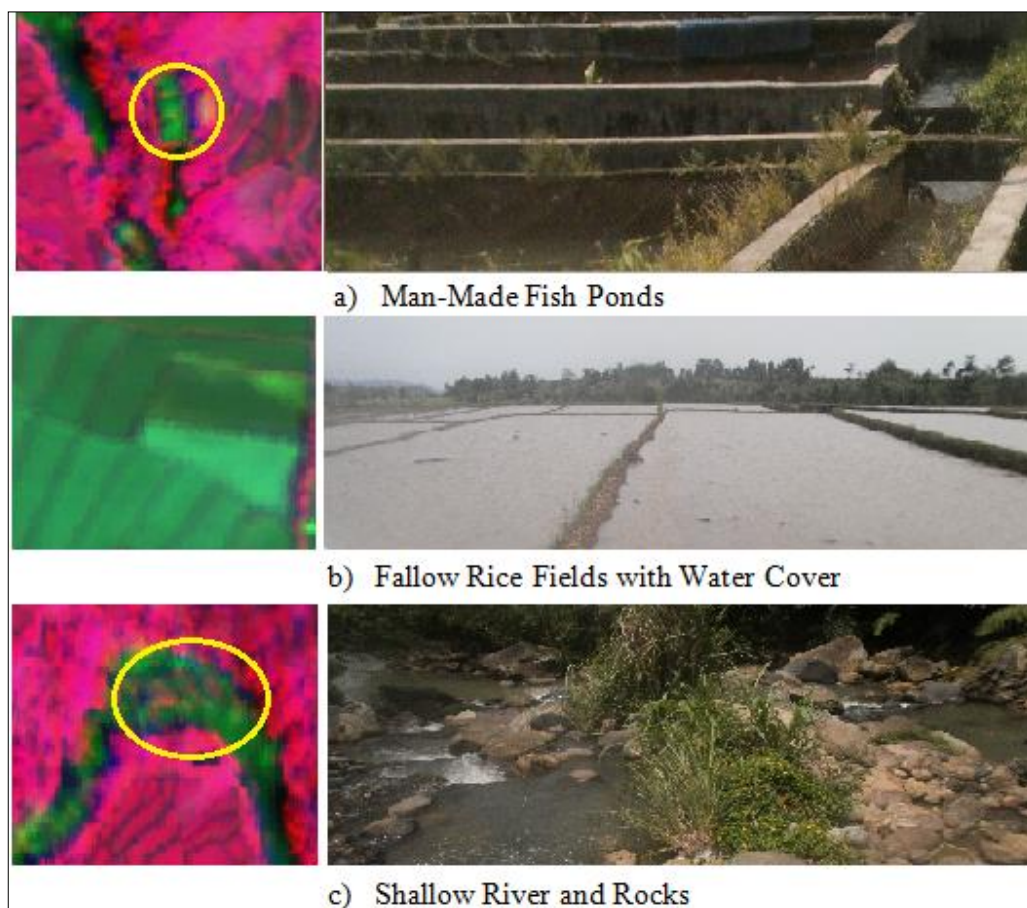
Figure 4-1   Fallow/Non Vegetation Class

In Figure 4-1, fallow/non vegetation class consists of various objects, such as fallow with water cover, fields' boundary, rocks, rivers, fish ponds, and another various objects with small area like grass in the river. Color of non vegetation in image maps can be distinguished easily with vegetation objects. Object without vegetation will be colored green and object with vegetation will be colored red.

New rice planting class is illustrated in Figure 4-2. Characteristics of new rice planting is has rare vegetation cover. With a resolution of around half meter, image color in the map is a combination of vegetative rice and fallow. The new rice planting class is early stages of paddy vegetative phase especially seeding until tillering stages (IRRI, 2012), due to the special characteristics of this object, it is classified separately.

Figure 4-2   New Rice Planting Class

Vegetative rice class is illustrated in Figure 4-3. A characteristic of vegetative rice is to have dense vegetation. Color on visual observation is green uniforms and a color in an image map is a red uniform.

Figure 4-3   Vegetative Rice Class

Reproductive rice class is illustrated in Figure 4-4. Color on visual observation in this stage is yellowish green. Characteristic of this phase at the time

of the survey is that the rice was still a flower.

Figure 4-4   Reproductive Rice Class

Ripening rice class is illustrated in Figure 4-5. Color on visual observation in this stage is dominantly yellow. Some land covers change during delay capture images and field survey (6 days) especially in this class. Some ripening rice changed to post harvest. This information obtained by interviewing farmers on the site.

Figure 4-5   Ripening Rice Class

Trees class is illustrated in Figure 4-6. The study areas there are several kinds of trees. Trees class can be detected by looking at the color, images pattern, and survey data.

Figure 4-6   Trees Class

4.2.1 Compilation of Data Set

Compilation of data set consists of training data and validating data. The accuracy assessment reference data must be kept absolutely independent (i.e., separate) from any training/labeling data (Congalton and Green, 1999). Each training and validating data consists of 3 input from original images (NIR, red, green), 13 inputs from image rationing as shown in Table 2-1, and target data for training or references data for validating. The selected training areas should be homogeneous as much as possible.

The examples of training and validating area are described in Figure 4-7. The images also show training targets and references validating each class. Those classes are derived from field observations and taking into account the spatial resolution of remote sensing data. The area of training data sets are represented by each class type selected based on the ground reference points collected from the field supported by the local knowledge of the area.
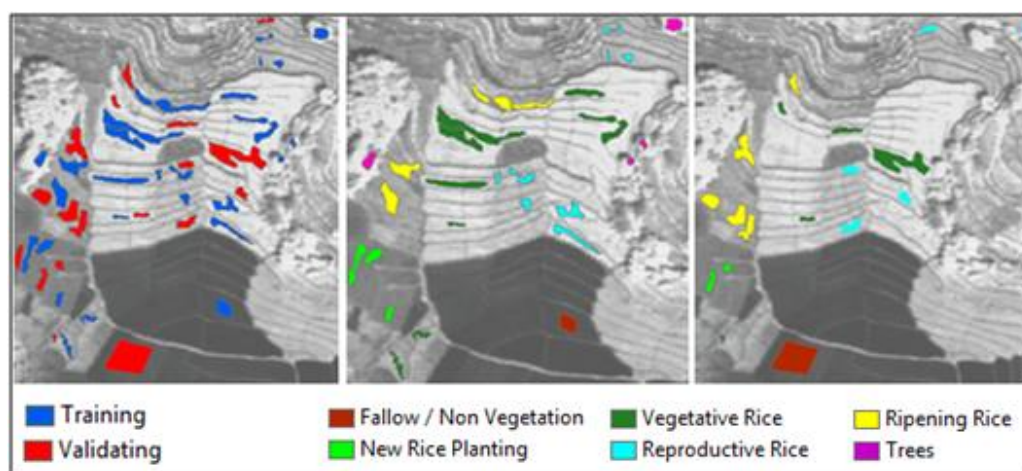
Figure 4-7   Examples of Training and Validating Area.

Validating and training samples used in this study are described in Table 4-2. Supervised classification methods are trained on labeled data. As the number of bands increase the number of training data for classification increase too. In usual case, the minimum number of training data for each class is 10N, where N is the number of bands (Salehi et al., 2004). In Table 4-2, the total number of samples per class is more than 30. It means that the amounts of sample data are more than enough to be used as training or validating. Example of data used in scenarios is shown in Appendix 2.

Table 4-2   Number of Validating and Training Samples

No	Class	Training (Pixel)	Validating (Pixel)
1	Fallow / Non Vegetation	3,226	5,125
2	New Rice Planting	1,062	716
3	Vegetative Rice	3,692	1,862
4	Reproductive Rice	1,062	720
5	Ripening Rice	2,436	3,779
6	Trees	1,742	455
	Total	13,220	12,657

4.3   Accuracy Assessment

4.3.1   Accuracy Assessment for Each Scenario

In this study, the same parameters have been used for each scenario. The parameters were three input and three membership functions (low, medium, and high), with epoch number = 1000, step size= 0.01, step size decrement Rate = 0.9, and step size increment rate = 1.1. Results of accuracy assessment for each scenario are described in Table 4-3.

Mather (2004) suggests that a value of kappa of 0.75 or greater shows a 'very good to excellent' classifier performance, while a value of less than 0.4 is 'poor'. Congalton and Green, (1999) characterized the possible ranges for KHAT (kappa) into three groups: a value greater than 0.80 represents strong agreement; a value between 0.4 and 0.8 represents moderate agreement; and a value below 0.40 represents poor agreement.

Best accuracy results occurred in scenario 22 with images rationing input (MPRI, NDVSI, and SAVI) with trapezoid fuzzy membership function, with kappa value of 95.76%. Worst accuracy results occurred in scenario 1 with input original image input (Red, Green, and NIR) with triangle fuzzy membership function, with kappa value of 30.85%.

Table 4-3   Scenario Comparison

Scenario	Variable Fuzzy			Membership Function	ANFIS RMSE	Training		Validating	
	X	Y	Z			OA	K	OA	K
1	Red	Green	NIR	Triangle	1.638	42.05	30.86	43.79	30.85
2	Red	Green	NIR	Trapezoid	0.45	74.41	68.5	60.61	49.39
3	Red	Green	NIR	Gaussian	0.388	83.53	79.43	66.3	56.64
4	Red	Green	NIR	General bell	0.387	84.01	80.03	53.84	43.41
5	RVI	RGRI	GRVI	Triangle	0.268	92.66	90.85	88.1	83.88
6	RVI	RGRI	GRVI	Trapezoid	0.246	94.48	93.1	94.86	92.84
7	RVI	RGRI	GRVI	Gaussian	0.255	93.12	91.42	90.87	87.51
8	RVI	RGRI	GRVI	General bell	0.218	95.05	93.83	94.68	92.63
9	NDVI	GNDVI	NDGRI	Triangle	0.351	87.82	84.85	89.1	84.89
10	NDVI	GNDVI	NDGRI	Trapezoid	0.367	89.11	86.35	92.06	88.93
11	NDVI	GNDVI	NDGRI	Gaussian	0.253	93.03	91.31	91.51	88.37
12	NDVI	GNDVI	NDGRI	General bell	0.242	93.71	92.17	93.62	91.15
13	EVI 2	OSAVI	SAVI	Triangle	0.554	79.65	74.48	85.57	79.84
14	EVI 2	OSAVI	SAVI	Trapezoid	0.515	82.44	78.37	90.9	87.41
15	EVI 2	OSAVI	SAVI	Gaussian	0.464	86.1	82.77	88.98	84.92
16	EVI 2	OSAVI	SAVI	General bell	0.442	89.7	87.21	92.6	89.82
17	RNDVI	MPRI	TNDVI	Triangle	0.392	79.75	74.9	78.49	71.11
18	RNDVI	MPRI	TNDVI	Trapezoid	0.289	91.87	89.91	92.99	90.29
19	RNDVI	MPRI	TNDVI	Gaussian	0.207	96.04	95.06	96.66	95.36
20	RNDVI	MPRI	TNDVI	General bell	0.238	94.07	92.6	94.03	91.72
21	MPRI	NDVSI	SAVI	Triangle	0.243	94.08	92.64	94	91.67
22	MPRI	NDVSI	SAVI	Trapezoid	0.212	**96.32**	**95.4**	**96.96**	**95.76**
23	MPRI	NDVSI	SAVI	Gaussian	0.212	96.07	95.09	96.47	95.09
24	MPRI	NDVSI	SAVI	General bell	0.211	95.88	94.86	95.98	94.42

* X:Variable Fuzzy 1, Y: Variable Fuzzy 2, Z: Variable Fuzzy 3,
OA: Overal Accuracy, K: Kappa %, Red Text: Best Value

From Table 4-3, the dominant factor causing low accuracy is the input factor while membership functions type does not have significant effect. For scenario number 1 to 4, all accuracies are under 60%, where those scenarios have the same input with different membership functions. Generally in this research, triangle membership function has the lowest accuracy. The best membership function type depends on input scenario. Trapezoid membership function is best for RVI/RGRI/GRVI and MPRI/NDVSI/SAVI input. Gaussian membership function is best for Red/Green/NIR and MDVI/MPRI/TNDVI input. General Bell membership function is best for NDVI/GNDVI/NDGRI and EVI2/OSAVI/SAVI input. The best scenario input can be seen on scenario 21 to 24 with MPRI/NDSVI/SAVI input. The final membership function comparison on best scenario is shown in Appendix 9.

One cause of low accuracy was due to the input statistics that were almost the same between classes. Input statistics of each class consisting of the average, minimum, maximum and standard deviation are shown in Appendix 3. From the data in Appendix 3 can be improved to normal distribution curve to see the possibility of different classes with the same value.

The normal distribution is a commonly occurring shape for population distributions. On normal distribution curve, the X axis represents different values for input, and the Y axis represents the density or the frequency or probability of occurrence of input. The total area under the curve is equal to 1. Normal distribution curve is shown in Appendix 4.

Normal distribution curve with red channel input overlapping occurs between ripening and new planting class. On green channel overlapping occurs between fallow with new planting class and ripening with trees class. On NIR channel overlapping occurs between ripening, trees, and vegetative class. These caused low accuracy in scenario 1 to 4.

4.3.2 Accuracy Assessment for Each Class

This section discusses the individual plant growth stages classes derived only from best scenario. The best scenario occurred from image rationing input. Accuracy assessment of each class is described in error matrix of training and error matrix of validating. Error on training matrix will create less precise Fuzzy Interference System (FIS) parameters to predict the targets from the input system. Error in the validation matrix demonstrates the ability of FIS to output predict which correspond to the actual class. Error matrix of training is described in Table 4-4 and Error matrix of validating is described in Table 4-5.

From Tables 4-4 and 4-5, the best class is the new rice planting and ripening rice with producer's accuracy of more than 97 % and user's accuracy of more than 99%, followed by the paddy vegetative with producer's accuracy of 93.98 % and user's accuracy of 97.58 %. The class that predicted the worse is the reproductive paddy with producer's accuracy of 78.61 % and user's accuracy of 74.38 %.

Table 4-4   Error Matrix of Training

Reference (Col) Prediction (Row)	Fallow /Non Veg	New Rice Planting	Vegetative Rice	Reproductive Rice	Ripening Rice	Trees	Total	UA (%)
Fallow /Non Veg	3226	0	0	0	0	0	3226	100
New Rice Planting	0	1050	0	0	0	0	1050	100
Vegetative Rice	0	11	3492	152	5	0	3660	95.41
Reproductive Rice	0	1	176	910	102	11	1200	75.83
Ripening Rice	0	0	19	0	2329	4	2352	99.02
Trees	0	0	5	0	0	1727	1732	99.71
Total	3226	1062	3692	1062	2436	1742	13220	
PA(%)	100	98.87	94.58	85.69	95.61	99.14		
Overal Accuracy (%)	:	96.32						
Kappa (x 100 %)	:	95.4						

Table 4-5   Error Matrix of Validating

Reference (Col) Prediction (Row)	Fallow /Non Veg	New Rice Planting	Vegetative Rice	Reproductive Rice	Ripening Rice	Trees	Total	UA (%)
Fallow /Non Veg	5125	0	0	49	0	1	5175	99.03
New Rice Planting	0	703	0	6	0	0	709	99.15
Vegetative Rice	0	13	1750	99	9	1	1872	93.48
Reproductive Rice	0	0	101	566	94	0	761	74.38
Ripening Rice	0	0	11	0	3676	1	3688	99.67
Trees	0	0	0	0	0	452	452	100
Total	5125	716	1862	720	3779	455	12657	
PA(%)	100	98.18	93.98	78.61	97.27	99.34		
Overal Accuracy (%)	:	96.96						
Kappa (x 100 %)	:	95.76						

In all normal distribution curves in Appendix 4, overlapping occurs between vegetative rice and reproductive rice class except in GNDVI. But in GNDVI overlapping occurs between reproductive with ripening class and vegetative with new planting class. On MPRI input, big overlapping only occurs between vegetative rice and reproductive rice class. These caused on reproductive rice and vegetative rice to have lower accuracy than ripening rice and new rice planting class. All inputs having similar the weakness, which clearly distinguishes between vegetative rice and reproductive rice. On NDVSI, big overlapping occurs between vegetative rice, reproductive rice, and trees class.

Although some overlapping kappa value was still high, the accuracy of each class was still greater than 70%. Two related studies have been conducted; the study modeled the relationship between vegetation index and age of rice plants using a temporal analysis. The first study, modeled EVI at the age of rice plants

using MODIS Data (Domiri et al., 2005). The second study, modeled NDVI at the age of rice plants using ASTER Data (Nugroho et al., 2008). Results from both studies are depicted in Figure 4-8.
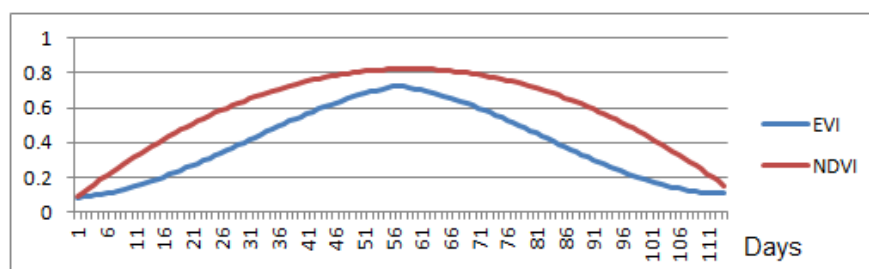
Figure 4-8   Vegetation Index of Rice from MODIS and ASTER

From Figure 4-8, vegetation index were possibly same value between before and after the 56 day. In the tropics, the reproductive phase is about 35 days and the ripening phase is about 30 days. The differences in growth duration are determined by changes in the length of the vegetative phase. For example, IR64 which matures in 110 days has a 45-day vegetative phase, whereas IR8 which matures in 130 days has a 65-day vegetative phase (IRRI, 2012). This was probably the cause of overlapping between vegetative, reproductive, and trees on the vegetation index such as NDVSI and SAVI.

Statistics on individual inputs have big overlapping values, but it did not occur on combination input. The relationship between the input data for each combination and the position of each class can be seen in a three-dimensional scattering graph. The 3-D scatter graph of training data is shown in Appendix 5. From Appendix 5 if viewed from each side with two input combinations, only small overlapping occurred. MPRI, NDVSI, and SAVI are generated from the derivative of original airborne line scanner (red, green, NIR). This means that the data from airborne line scanner is quite good for rice plant growth stage mapping.

From Table 4-3, the whole scenario with the image rationing input had kappa values of more than 70%. This means that the ANFIS method is good enough to rice plant growth stage mapping from airborne line scanner.

4.3 Best Scenario of ANFIS Training

ANFIS uses a hybrid learning algorithm to identify parameters of fuzzy inference systems type 3. During the learning process, every epoch has RMS error and updates the step size. Error and step size curve are described in Figure 4-9.
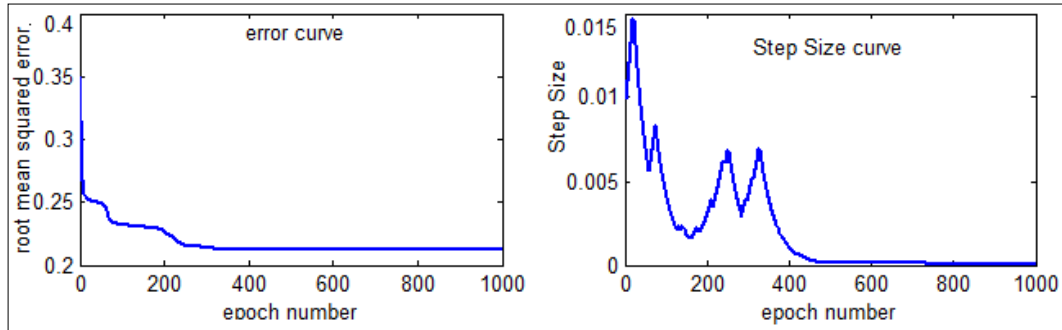
Figure 4-9   Error and Step Size Curve

After the ANFIS learning process, premise and consequent parameters will be generated. Premise parameter is a parameter of membership degree which depend type of membership function. The initial value of membership function is calculated based on the statistics of the input training data. Final membership function is calculated based on ANFIS algorithm from input and target of training data. Initial and final membership function is described in Figure 4-10 and parameter of final membership function is described in Table 4-6.
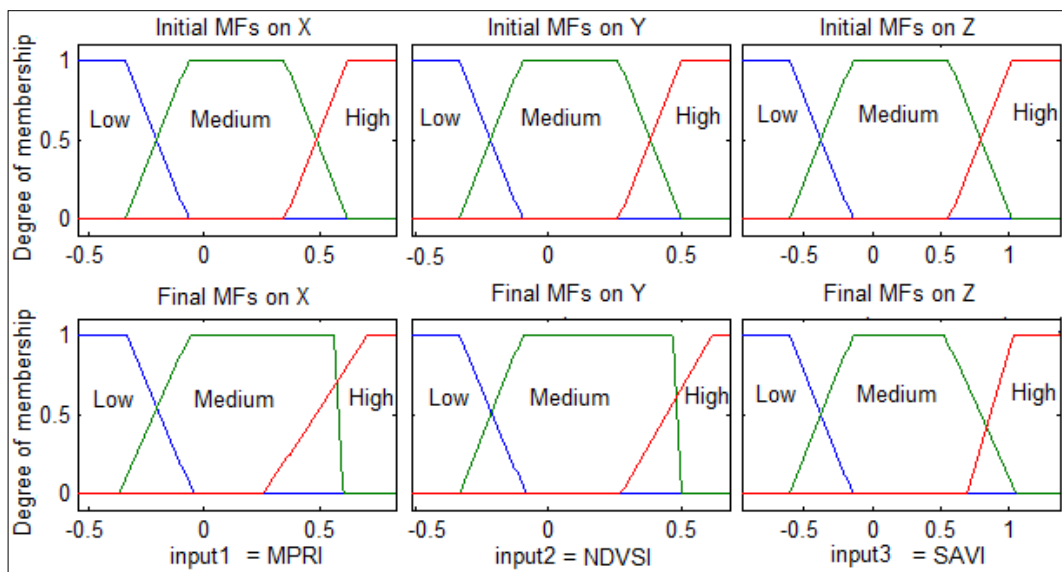
Figure 4-10 Initial and Final Membership Function

Table 4-6   Parameter of Membership Function

Variable Fuzzy	Membership function											
	Low				Medium				High			
	a	b	c	d	a	b	c	d	a	b	c	d
MPRI (X)	-1.024	-0.750	-0.333	-0.046	-0.367	-0.060	0.557	0.596	0.254	0.705	1.027	1.301
NDVSI (Y)	-0.935	-0.695	-0.334	-0.083	-0.334	-0.095	0.469	0.502	0.272	0.622	0.863	1.102
SAVI (Z)	-1.781	-1.313	-0.608	-0.142	-0.609	-0.139	0.532	1.065	0.694	1.044	1.734	2.203

In FIS type 3, the consequent is a crisp function of the antecedent variables. Fuzzy IF-THEN rule is a concept used for describing of logical dependence between variables of premise and consequent part. Rule and consequent parameters from best scenario is described in Table 4-7.

Table 4-7   Rule and Consequent Parameter

No	Rule of Fuzzy Interferences System								
	Premise Part			Consequent Part					
1	If X is Low	& Y is Low	& Z is Low	Then f1 =	0.2 X +	0.8 Y -	0.6 Z +	0.9
2	If X is Low	& Y is Low	& Z is Medium	Then f2 =	26.8 X -	9.2 Y +	11.3 Z +	15.8
3	If X is Low	& Y is Low	& Z is High	Then f3 =	0.0 X +	0.0 Y +	0.0 Z +	0.0
4	If X is Low	& Y is Medium	& Z is Low	Then f4 =	11.2 X +	34.6 Y -	24.1 Z -	0.3
5	If X is Low	& Y is Medium	& Z is Medium	Then f5 =	29.8 X +	128.4 Y -	84.8 Z -	7.6
6	If X is Low	& Y is Medium	& Z is High	Then f6 =	0.0 X +	0.0 Y +	0.0 Z +	0.0
7	If X is Low	& Y is High	& Z is Low	Then f7 =	0.0 X +	0.0 Y +	0.0 Z +	0.0
8	If X is Low	& Y is High	& Z is Medium	Then f8 =	0.0 X +	0.0 Y +	0.0 Z +	0.0
9	If X is Low	& Y is High	& Z is High	Then f9 =	0.0 X +	0.0 Y +	0.0 Z +	0.0
10	If X is Medium	& Y is Low	& Z is Low	Then f10 =	8.9 X -	6.4 Y -	2.6 Z -	0.2
11	If X is Medium	& Y is Low	& Z is Medium	Then f11 =	53.8 X -	16.3 Y +	0.9 Z +	2.1
12	If X is Medium	& Y is Low	& Z is High	Then f12 =	0.0 X +	0.0 Y +	0.0 Z +	0.0
13	If X is Medium	& Y is Medium	& Z is Low	Then f13 =	3.1 X +	25.0 Y -	21.0 Z -	1.0
14	If X is Medium	& Y is Medium	& Z is Medium	Then f14 =	-20.8 X -	35.7 Y +	22.2 Z +	2.9
15	If X is Medium	& Y is Medium	& Z is High	Then f15 =	400.4 X +	845.7 Y -	670.2 Z +	86.7
16	If X is Medium	& Y is High	& Z is Low	Then f16 =	0.0 X +	0.0 Y +	0.0 Z +	0.0
17	If X is Medium	& Y is High	& Z is Medium	Then f17 =	-416.4 X -	948.5 Y +	650.5 Z -	7.8
18	If X is Medium	& Y is High	& Z is High	Then f18 =	50.9 X +	96.5 Y -	109.3 Z +	45.8
19	If X is High	& Y is Low	& Z is Low	Then f19 =	0.0 X +	0.0 Y +	0.0 Z +	0.0
20	If X is High	& Y is Low	& Z is Medium	Then f20 =	0.0 X +	0.0 Y +	0.0 Z +	0.0
21	If X is High	& Y is Low	& Z is High	Then f21 =	0.0 X +	0.0 Y +	0.0 Z +	0.0
22	If X is High	& Y is Medium	& Z is Low	Then f22 =	0.0 X +	0.0 Y +	0.0 Z +	0.0
23	If X is High	& Y is Medium	& Z is Medium	Then f23 =	-5.0 X -	116.3 Y +	573.2 Z -	367.1
24	If X is High	& Y is Medium	& Z is High	Then f24 =	27.8 X +	20.6 Y -	28.5 Z +	11.2
25	If X is High	& Y is High	& Z is Low	Then f25 =	0.0 X +	0.0 Y +	0.0 Z +	0.0
26	If X is High	& Y is High	& Z is Medium	Then f26 =	26.3 X +	224.6 Y +	32.7 Z -	222.8
27	If X is High	& Y is High	& Z is High	Then f27 =	10.4 X +	8.7 Y -	14.3 Z +	11.9

Using the parameters in Tables 4.6 and 4.7 and using the formula FIS type 3 or ANFIS, which described in Section 2.3.2, all pixels in the image to be predicted output value. Output value is still floating number; small possibility the

output value is exactly same as the target value of the class, except for the ANFIS training - RMS error is zero. To convert the float number to integer, range value is required. Target and range value of the class is described in the Table 4-8.

Table 4-8   Target and Range Value

Class Name	Fallow / Non Vegetation	New Rice Planting	Vegetative Rice	Reproductive Rice	Ripening Rice	Trees
Class Value	1	2	3	4	5	6
Range Value (F)	< 1.5	1.5 - 2.5	2.5 - 3.5	3.5 - 4.5	4.5 - 5.5	> 5.5

After this process, the best scenario of ANFIS training for plant growth stage mapping was obtained. The best scenario of ANFIS training for plant growth stage mapping is shown in Appendix 6. The sample calculation of best scenario is shown in Appendix 7.

4.4   Rice Plant Growth Stage Mapping

Before calculating the area of rice plant growth stage, error correction should be done that cannot be avoided in automatic classification. Often, fully automated algorithms produce incomplete results so that manual post processing is inevitable (Kim et al., 2005). This section discusses the methods of classification results improved by giving a value to each segment based on the majority class. Object instance is vegetation rice in study area. The object is depicted in Figure 4-11.

Figure 4-11 Photo Survey of Vegetative Rice

Photo survey in Figure 4-11 in images is described in Figures 4-12. From the image, the boundary of each field is clearly visible, so that manual segmentation can be done. Each segment has an identification number (ID).

Figure 4-12 Post Processing

From the Figure 4-12, the results of classification still have errors such as ripening and reproductive rice. After class majority segment is used, each segment has one result. Calculation of majority class of each segment is described in Table 4-9.

From table 4-9, the number of pixel of each segment is calculated. Then for each segment, the number of pixel of each class is calculated to determine the class with the most number of pixel. Finally every pixel in that segment is transformed into the class with most number of pixel.

Table 4-9   Statistic of Majority Class

ID	Majority class	% Majority	% Fallow	% New	% Vegetative	% Reproductive	% Ripening	% Trees
403	Vegetative	55.86	0.00	0.00	55.86	37.54	6.61	0.00
411	Vegetative	60.85	3.23	2.45	60.85	12.92	20.54	0.00
418	Vegetative	62.05	0.00	0.00	62.05	27.85	10.10	0.00
421	Vegetative	44.71	0.00	0.32	44.71	18.80	36.18	0.00
422	Vegetative	63.68	0.00	0.10	63.68	35.56	0.67	0.00
423	Vegetative	70.20	0.00	0.49	70.20	28.08	1.23	0.00
431	Vegetative	60.22	0.00	0.00	60.22	33.70	6.09	0.00
436	Vegetative	63.87	0.21	0.56	63.87	29.91	5.45	0.00
445	Vegetative	77.55	0.00	3.01	77.55	18.06	1.39	0.00
446	Vegetative	69.16	0.00	0.00	69.16	28.19	2.64	0.00
455	Vegetative	72.03	0.00	0.21	72.03	19.71	8.05	0.00
458	Vegetative	58.98	0.00	0.07	58.98	32.85	8.09	0.00
462	Vegetative	63.22	0.00	3.51	63.22	30.58	2.69	0.00
464	Vegetative	74.35	0.00	0.70	74.35	23.44	1.51	0.00
472	Vegetative	67.40	0.00	0.00	67.40	31.94	0.66	0.00
473	Vegetative	71.94	0.00	0.00	71.94	23.84	4.22	0.00
475	Vegetative	62.52	0.00	0.00	62.52	19.79	17.69	0.00
477	Vegetative	47.50	0.00	0.18	47.50	42.88	9.43	0.00
479	Vegetative	94.81	0.35	0.00	94.81	4.15	0.35	0.35

The study area has been segmented as many as 1,172 pieces, with majority class average of 64.17%. Details of majority percentage of each segment are described in Figure 4-13. In Figure 4-13 has been sequenced from fallow class until trees class. Each class has been sorted from smallest to largest majority.
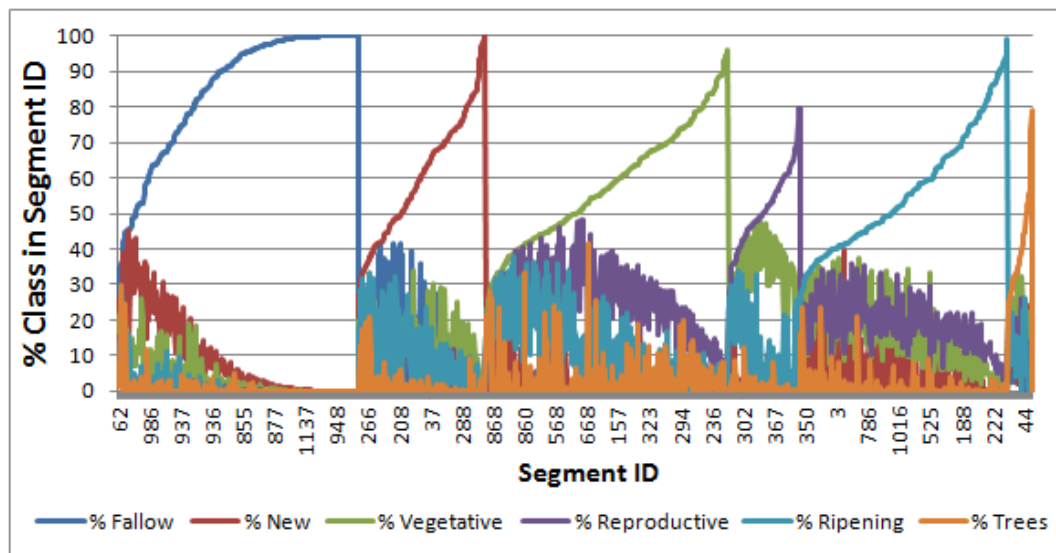
Figure 4-13 Majority Class Each Segment

Map and result of rice plant growth stage were obtained after post processing. Results of plant growth stage mapping are described in Table 4-10. Plant growth stage mapping is shown in Appendix 8.

Table 4-10   Result of Plant Growth Stage Mapping

No	Class	number of segments	Pixel	Area(Ha)
1	Fallow / Non Vegetation	310	594,234	13.01
2	New Rice Planting	162	178,390	3.91
3	Vegetative Rice	311	307,045	6.72
4	Reproductive Rice	92	97,311	2.13
5	Ripening Rice	266	343,384	7.52
6	Trees	31	619,914	13.57
	total	1172	2,140,278	46.85

V. CONCLUSIONS AND RECOMMENDATIONS

5.1 Conclusions

The classification method have been developed using airborne line scanner data and ANFIS algorithm. This method has been applied to plant growth stage mapping. Data from airborne line scanner is quite good for distinguish of rice plant growth stage. ANFIS method is good enough to rice plant growth stage mapping from airborne line scanner.

Best accuracy results occurred in scenario with input images rationing (MPRI, NDVSI, and SAVI) with trapezoid fuzzy membership function, which gives kappa value 95.76%.

The predicted best class is paddy new planting and paddy ripening with producer's accuracy of more than 97 % and user's accuracy of more than 99% followed by paddy vegetative with producer's accuracy of 93.98 % and user's accuracy of 97.58 %. The class that predicted worse is paddy reproductive with producer's accuracy of 78.61 % and user's accuracy of 74.38 %.

5.2 Recommendations

Based on result there are several issues that can be further investigating to improve the results:

1. It may be worthy investigating different membership function in ANFIS.
2. It needs to compare with the result of applying the method to different sensor with different spatial resolution, so that the accuracy obtained is more comprehensive.
3. Improvement may be obtained by combining the image and environmental data and compared with images rationing using the ANFIS method.
4. It is need for further researches to explore the ANFIS method for automatic image segmentation and combined with classification based on color.

REFERENCES

Abrams, J.M., 1983, Remote sensing for porphyry copper deposits in Southern Arizona. *Economic Geology*, 78, pp.591-604.

Salehi B.M. J., Valadan Zouj, 2004, Wavelet Spectral Analysis for Automatic Reduction of Hyperspectral Imagery , http://www.gisdevelopment.net/technology/ip/mi04013.htm

Bertels, L., Deronde, B., Kempeneers, P., Provoost, S., Tortelboom, E., 2005; Potentials of airborne hyperspectral remote sensing for vegetation mapping of spatially heterogeneous dynamic dunes, a case study along the Belgian coastline; *Interantional Conference on Nature Resporation Practices in European Coastal Habitats*, Koksijde, Belgium, pp 153-163.

Calado, T.J., DaCamara, C.C. 2006, A synergetic use of remote-sensed data to assess the evolution of burnt area by wildfires in Portugal. *The 2006 EUMETSAT Meteorological Satellite Conference*, Helsinki, Finland, 12-16 June 2006, EUMETSAT P.48, ISBN 92-9110-076-5, 8pp

Congalton RG, Green K. 1999. *Assesing the Accuracy of Remotely Sensed Data: Principle and Practices*. New York:CRC Press, Inc.

Corucci Linda, Masini Andrea, 2010, Oil spill classification from multi-spectral satellite images using a neuro-fuzzy technique, *IEEE GOLD Remote Sensing Conference*, pp 1-3, Livorno, Italy.

Crane, R. B., 1971. Processing techniques to reduce atmospheric and sensor variability in multispectral scanner data. *Proceed 7th. Int. Symp. Remote Sens. Environ.*, Ann Arbor, Vol.2, pp. 1345-1355

Dadhwal, V.K., 2004, Crop growth and productivity monitoring and simulation using remote sensing and GIS, Satellite RS and GIS Application in *Agriculture Meteorology*, pp. 263-289.

Domiri D.D., Adhyani N.L.,Nugraheni S., 2005, Rice plant growth model using MODIS data for rice age prediction,Prosiding Pertemuan Ilmiah Tahunan MAPIN XIV, ISBN : 979-98982-1-8. pp 17-23.

Efendigil, T., S. Onut, C. Kahraman, 2009, A decision support system for demand forecasting with artificial neural networks and neuro-fuzzy models: A comparative analysis, *Expert Systems with Applications*, volume 36, number 3, April 2009: 6697-6707.

Fletcher, R.S.; Everitt, J.H.; Elder, H.S. 2010, Evaluating Airborne Multispectral Digital Video to Differentiate Giant Salvinia from Other Features in Northeast Texas. *Remote Sensing*. 2010, 2, 2413-2423.

Gitelson, A.A., Y.J. Kaufman, and M.N. Merzlyak, 1996. Use of a green channel in remote sensing of global vegetation from EOS-MODIS, *Remote Sensing Environment*, 58:289-298.

Gong P., Biging G.S., Larrieu M.R., 2003. Estimation of forest leaf area index using vegetation indices derived from hyperion hyperspectral data, *IEEE Trans. on Geoscience and Remote Sensing*, Vol. 41, No. 6, June 2003.

Hatfield J.L. Prueger J.H., 2010. Value of Using Different Vegetative Indices to Quantify Agricultural Crop Characteristics at Different Growth Stages under Varying Management Practices. *Remote Sensing*. Vol.2, no. 2: 562-578.

Huete, A. R., 1988. A soil-adjusted vegetation index (SAVI), *Remote Sensing of Environment*, 25, 53-70.

Imdad A.R., Mohan B.K., 2010, Improving The Accuracy Of Object Based Supervised Image Classification Using Cloud Basis Functions Neural Network For High Resolution Satellite Images, *International Journal Of Image Processing*, ISSN 1985-2304 Volume 4.

IRRI [Internet]. 2012. International Rice Research Institute, Available:http://www.knowledgebank.irri.org/extension/three-growth-phases.html. Accessed July 2, 2012

Jang S.R., 1993, ANFIS: Adaptive-Network-based Fuzzy Inference Systems, *IEEE Transactions on Systems, Man, and Cybernetics*, Vol. 23, No. 3, pp. 665-685.

Jiang Z., Huete A.R., Youngwook K., Kamel D., 2007. 2-band enhanced vegetation index without a blue band and its application to AVHRR data, *Proc. SPIE, Remote Sensing and ModelingTheory, Techniques, And Applications I*, Vol. 6679, 667905.

Jordan, C.F., 1969. Derivation of leaf-area index from quality of light on the forest floor, *Ecology*, 50, pp. 663-666.

Brown K., 2004, Increasing classification accuracy of coastal habitats using integrated airborne remote sensing. *EARSeL Proceedings*, 2004, vol.3, pp.34-42

Kim T, Park S.R, Kim M.G, Jeong S, Kim K.O, 2005, Tracking road centerlines from high resolution remote sensing images by least squares correlation matching. *Photogrammetric Engineering & Remote Sensing* 70(12), 1417-1422.

Lillesand,T.M. and Kiefer,R.W, 1979, *Remote Sensing and Image Interpretation, NewYork,* Wiley. 2nd edition.

Mather P.M. 2004. *Computer Processing of Remotely-Sensed Images* . London: John Wiley & Sons Ltd

Monireh S.H. and Maryam Z., 2012, A review of medical image classification using Adaptive Neuro-Fuzzy Inference System (ANFIS), *Journal of Medical Signal and Sensors* Vol 2 No1

Nugroho D.A., Sukojo B.M., Wahyudi Y., 2008. Rice plants Identification with convert radians to the reflectance data in ASTER image, *Prosiding Pertemuan Ilmiah Tahunan MAPIN XVII*, ISBN: 978-979-25-8362-5. pp 117-130.

Panuju D.R., Trisasongko B.H, 2008, The Use Of Statistical Tree Methods On Rice Field Mapping, *Jurnal ilmiah Geomatika* Vol. 14 No.2, Bakosurtanal, Desember 2008

Patil V.C,Maru A, Shashidhara G.B. and U.K.Shanwad, 2002. Remote Sensing, Geographical Information System and Precision Farming in India: Opportunities and Challenges. http://www.jsai.or.jp/afita/afita-conf/2002/part6/p478.pdf pp 1-9

Reulke R., Wehr A., Griesbach D,2004, High Resolution Mapping Using CCD-line Camera and Laser Scanner with Integrated Position and Orientation System , *International Society for Photogrammetric and Remote Sensing* volume XXXV, p. 506.

Rondeaux, G., M. Steven and F. Baret, 1996. Optimization of soil-adjusted vegetation indices, *Remote Sensing of Environment*, 55, pp.95-107.

Rouse, J. W., R. H. Haas, J. A. Schell, and D. W. Deering, 1973. Monitoring vegetation systems in the Great Plains with ERTS, *Third ERTS Symposium, NASA SP-351 I*, pp. 309-317.

Salem F., M. Kafatos, T. El-Ghazawi, R. Gomez, R. Yang, 2005. *Hyperspectral image assessment of oil-contaminated wetland, International Journal Remote Sensing.*, Vol. 26, N 4, pp. 811-821

Samaniego.L, Bardossy.A, Schulz.k, 2008, Supervised Classification of Remotely

Sensed Imagery Using a Modified -NN Technique, *IEEE Trans Geosci Remote Sensing* 46(7):2112-2125.

Santhosh B. and Devi M.R., 2011, Geometric Correction in Recent High Resolution Satellite Imagery: A Case Study in Coimbatore, Tamil Nadu. *International Journal of Computer Applications* 14(1):32-37, January 2011. Published by Foundation of Computer Science.

Stathakis D., SavinI.Yu., 2006. Neuro-fuzzy Modeling for Crop Yield Prediction, in the *Proc. Of ISPRS Mid-term Symposium 2006 Remote Sensing: From Pixels to Processes Enschede The Netherlands*.

Theta Aerospace, 2010, LAPAN LISA EM Glossary Training, LAPAN Internal Document.

Tjahjono B., A.H.A. Syafril, D.R. Panuju, A. Kasno, B.H. Trisasongko, F. Heidina, 2009, Rice field monitoring using ALOS AVNIR-2, *Jurnal Ilmiah Geomatika*, Vol 15 No.2, Bakosurtanal, Desember 2009

Tucker C.J., 1979. Red and photographic infrared linear combinations for monitoring vegetation, *Remote Sensing of Environment*, Vol. 8, pp. 127-150.

Wertz, James R.; Wiley J. Larson (1999). *Space Mission Analysis and Design* (3rd Ed. ed.). Kluwer Academic Publishers. ISBN 1-881883-10-8.

Yang Z, Willis P, Mueller R., 2008. Impact of band-ratio enhanced AWIFS image to crop classification accuracy, The Future of Land Imaging Going Operational, *The 17th William T. Pecora Memorial Remote Sensing Symposium*, Denver, Colorado.

Yu, Q., P. Gong, N. Clinton,G. Biging, M. Kelly and D. Schirokauer, 2006, Object-based detailed vegetation classification with airborne high spatial resolution remote sensing imagery, *Photogrammetric Engineering and Remote Sensing*, 72(7) 799-811

Appendix 1   Corrected Image of Airborne Line Scanner

45
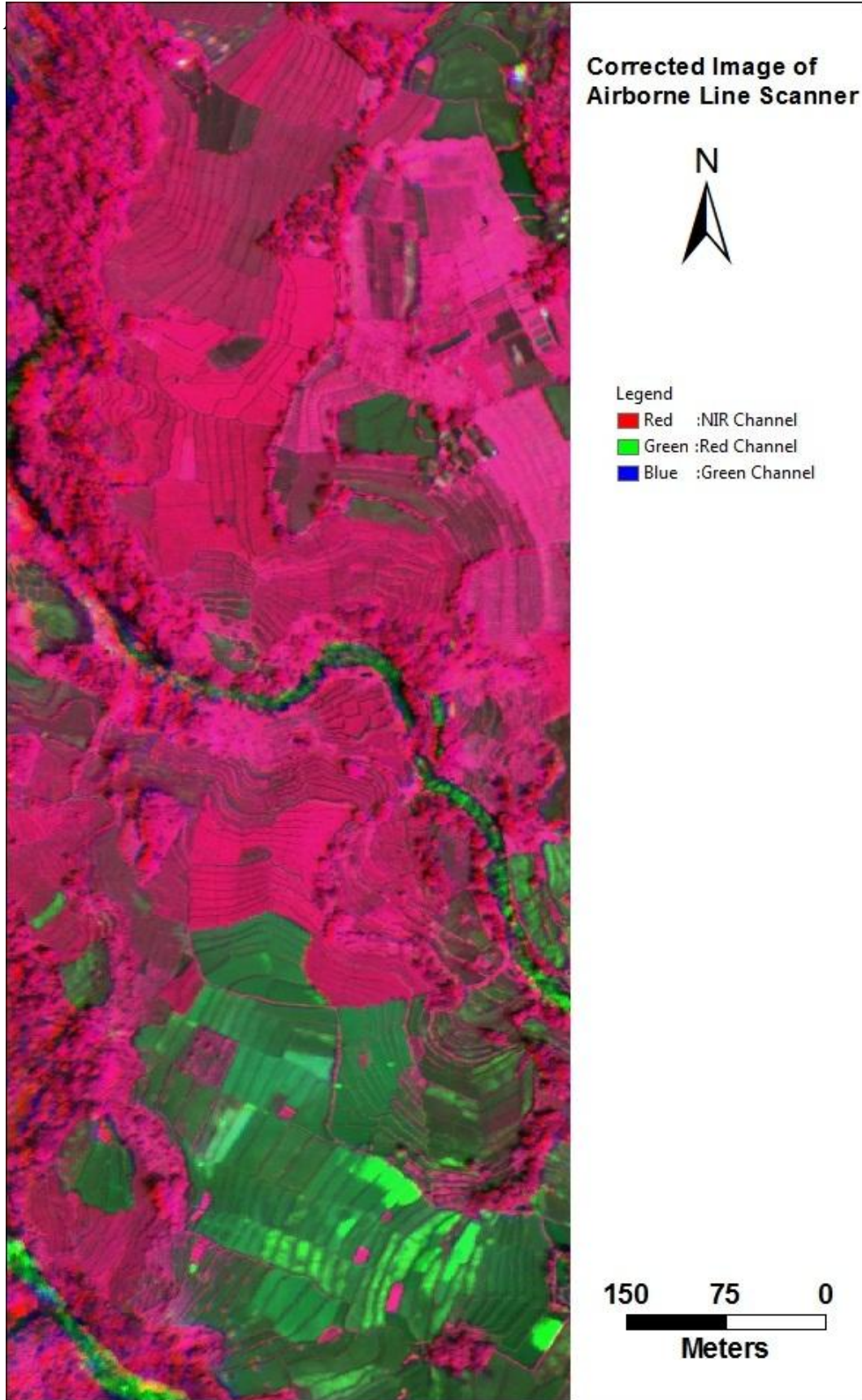
Appendix 2   Example of Data Used in Scenario

No	Nir	Red	Green	RNDVI	MPRI	NDVI	EVI2	RVI	RGRI	GNDVI	NDGRI	NDVSI	TNDVI	GRVI	OSAVI	SAVI
						Class Name: Fallow/Non Vegetation										
1	5990	23908	7039	0.06	-0.55	-0.60	-1.50	0.25	3.40	-0.08	1.29	-0.44	0.63	0.85	-0.60	-0.90
2	4941	17826	7615	0.08	-0.40	-0.57	-1.41	0.28	2.34	-0.21	0.81	-0.44	0.66	0.65	-0.57	-0.85
3	5233	18738	7835	0.08	-0.41	-0.56	-1.41	0.28	2.39	-0.20	0.83	-0.43	0.66	0.67	-0.56	-0.85
4	5295	19321	7286	0.08	-0.45	-0.57	-1.42	0.27	2.65	-0.16	0.96	-0.43	0.66	0.73	-0.57	-0.85
5	5298	21400	7658	0.06	-0.47	-0.60	-1.51	0.25	2.79	-0.18	1.06	-0.47	0.63	0.69	-0.60	-0.90
6	14788	24460	12550	0.37	-0.32	-0.25	-0.62	0.60	1.95	0.08	0.44	-0.11	0.87	1.18	-0.25	-0.37
7	15595	24720	12473	0.40	-0.33	-0.23	-0.57	0.63	1.98	0.11	0.44	-0.09	0.88	1.25	-0.23	-0.34
8	15503	24796	12552	0.39	-0.33	-0.23	-0.58	0.63	1.98	0.11	0.44	-0.09	0.88	1.24	-0.23	-0.35
9	15617	25119	12742	0.39	-0.33	-0.23	-0.58	0.62	1.97	0.10	0.44	-0.10	0.88	1.23	-0.23	-0.35
10	15388	24460	12742	0.40	-0.31	-0.23	-0.57	0.63	1.92	0.09	0.42	-0.09	0.88	1.21	-0.23	-0.34
11	12649	20191	11991	0.39	-0.25	-0.23	-0.57	0.63	1.68	0.03	0.33	-0.12	0.88	1.05	-0.23	-0.34
12	13380	20575	11200	0.42	-0.30	-0.21	-0.53	0.65	1.84	0.09	0.38	-0.09	0.89	1.19	-0.21	-0.32
13	8979	30937	12471	0.08	-0.43	-0.55	-1.38	0.29	2.48	-0.16	0.86	-0.41	0.67	0.72	-0.55	-0.83
14	9006	30302	12577	0.09	-0.41	-0.54	-1.35	0.30	2.41	-0.17	0.82	-0.41	0.68	0.72	-0.54	-0.81
15	8829	30598	12299	0.08	-0.43	-0.55	-1.38	0.29	2.49	-0.16	0.87	-0.42	0.67	0.72	-0.55	-0.83

No	Nir	Red	Green	RNDVI	MPRI	NDVI	EVI2	RVI	RGRI	GNDVI	NDGRI	NDVSI	TNDVI	GRVI	OSAVI	SAVI
						Class Name: New Rice Planting										
1	29923	12241	14444	5.97	0.08	0.42	1.05	2.44	0.85	0.35	-0.05	0.38	1.19	2.07	0.42	0.63
2	29481	13331	14388	4.89	0.04	0.38	0.94	2.21	0.93	0.34	-0.02	0.36	1.17	2.05	0.38	0.57
3	28894	12858	13893	5.05	0.04	0.38	0.96	2.25	0.93	0.35	-0.02	0.37	1.18	2.08	0.38	0.58
4	28804	12858	13893	5.02	0.04	0.38	0.96	2.24	0.93	0.35	-0.02	0.37	1.18	2.07	0.38	0.57
5	28598	12248	13462	5.45	0.05	0.40	1.00	2.33	0.91	0.36	-0.03	0.38	1.18	2.12	0.40	0.60
6	33108	12057	14092	7.54	0.08	0.47	1.17	2.75	0.86	0.40	-0.04	0.43	1.21	2.35	0.47	0.70
7	29665	12676	14296	5.48	0.06	0.40	1.00	2.34	0.89	0.35	-0.04	0.37	1.18	2.08	0.40	0.60
8	28824	12934	14296	4.97	0.05	0.38	0.95	2.23	0.90	0.34	-0.03	0.36	1.17	2.02	0.38	0.57
9	29134	12766	14271	5.21	0.06	0.39	0.98	2.28	0.89	0.34	-0.03	0.37	1.18	2.04	0.39	0.59
10	30917	11555	14547	7.16	0.11	0.46	1.14	2.68	0.79	0.36	-0.07	0.41	1.21	2.13	0.46	0.68
11	27293	13515	14067	4.08	0.02	0.34	0.84	2.02	0.96	0.32	-0.01	0.33	1.16	1.94	0.34	0.51
12	26849	13757	13534	3.81	-0.01	0.32	0.81	1.95	1.02	0.33	0.01	0.33	1.15	1.98	0.32	0.48
13	27957	13286	13693	4.43	0.02	0.36	0.89	2.10	0.97	0.34	-0.01	0.35	1.16	2.04	0.36	0.53
14	27470	13945	13608	3.88	-0.01	0.33	0.82	1.97	1.02	0.34	0.01	0.33	1.15	2.02	0.33	0.49
15	30091	12430	14054	5.86	0.06	0.42	1.04	2.42	0.88	0.36	-0.04	0.39	1.19	2.14	0.42	0.62

No	Nir	Red	Green	RNDVI	MPRI	NDVI	EVI2	RVI	RGRI	GNDVI	NDGRI	NDVSI	TNDVI	GRVI	OSAVI	SAVI
						Class Name: Vegetative Rice										
1	44409	9327	16816	22.66	0.29	0.65	1.63	4.76	0.55	0.45	-0.12	0.55	1.29	2.64	0.65	0.98
2	40371	8352	16623	23.35	0.33	0.66	1.64	4.83	0.50	0.42	-0.15	0.53	1.29	2.43	0.66	0.99
3	40777	7941	16350	26.35	0.35	0.67	1.69	5.13	0.49	0.43	-0.15	0.54	1.29	2.49	0.67	1.01
4	42277	7735	16520	29.85	0.36	0.69	1.73	5.47	0.47	0.44	-0.15	0.55	1.30	2.56	0.69	1.04
5	51729	7556	18390	46.83	0.42	0.75	1.86	6.85	0.41	0.48	-0.15	0.60	1.32	2.81	0.75	1.12
6	50386	7150	18130	49.61	0.43	0.75	1.88	7.05	0.39	0.47	-0.16	0.60	1.32	2.78	0.75	1.13
7	52967	7336	18172	52.08	0.42	0.76	1.89	7.22	0.40	0.49	-0.15	0.61	1.33	2.91	0.76	1.14
8	52191	6746	17984	59.79	0.45	0.77	1.93	7.74	0.38	0.49	-0.16	0.62	1.33	2.90	0.77	1.16
9	53065	6502	22060	66.52	0.54	0.78	1.95	8.16	0.29	0.41	-0.21	0.58	1.33	2.41	0.78	1.17
10	53036	6325	21405	70.22	0.54	0.79	1.97	8.39	0.30	0.42	-0.20	0.59	1.34	2.48	0.79	1.18
11	53193	5865	21103	82.13	0.57	0.80	2.00	9.07	0.28	0.43	-0.21	0.60	1.34	2.52	0.80	1.20
12	52503	5684	18619	85.18	0.53	0.80	2.01	9.24	0.31	0.48	-0.18	0.62	1.34	2.82	0.80	1.21
13	53119	5397	19024	96.69	0.56	0.82	2.04	9.84	0.28	0.47	-0.19	0.63	1.35	2.79	0.82	1.22
14	53193	5311	19067	100.12	0.56	0.82	2.05	10.02	0.28	0.47	-0.19	0.63	1.35	2.79	0.82	1.23
15	51447	4735	19374	117.78	0.61	0.83	2.08	10.87	0.24	0.45	-0.21	0.62	1.35	2.66	0.83	1.25

Appendix 2   (Continued)

No	Nir	Red	Green	RNDVI	MPRI	NDVI	EVI2	RVI	RGRI	GNDVI	NDGRI	NDVSI	TNDVI	GRVI	OSAVI	SAVI
							Class Name: Reproductive Rice									
1	44766	8459	17081	27.99	0.34	0.68	1.71	5.29	0.50	0.45	-0.14	0.56	1.30	2.62	0.68	1.02
2	44425	7114	16626	38.96	0.40	0.72	1.81	6.24	0.43	0.46	-0.16	0.58	1.31	2.67	0.72	1.09
3	53128	9210	20829	33.25	0.39	0.70	1.76	5.77	0.44	0.44	-0.16	0.56	1.31	2.55	0.70	1.06
4	53128	8677	21033	37.46	0.42	0.72	1.80	6.12	0.41	0.43	-0.17	0.56	1.31	2.53	0.72	1.08
5	39811	6271	15538	40.26	0.42	0.73	1.82	6.35	0.40	0.44	-0.17	0.57	1.31	2.56	0.73	1.09
6	41369	6690	14861	38.20	0.38	0.72	1.80	6.18	0.45	0.47	-0.15	0.59	1.31	2.78	0.72	1.08
7	53738	8215	20435	42.76	0.43	0.73	1.84	6.54	0.40	0.45	-0.16	0.58	1.32	2.63	0.73	1.10
8	53738	8446	20334	40.45	0.41	0.73	1.82	6.36	0.42	0.45	-0.16	0.58	1.31	2.64	0.73	1.09
9	53738	8692	20432	38.20	0.40	0.72	1.80	6.18	0.43	0.45	-0.16	0.57	1.31	2.63	0.72	1.08
10	49550	7470	19000	43.96	0.44	0.74	1.84	6.63	0.39	0.45	-0.17	0.58	1.32	2.61	0.74	1.11
11	48422	8455	19565	32.78	0.40	0.70	1.76	5.73	0.43	0.42	-0.16	0.55	1.30	2.47	0.70	1.05
12	48620	8455	19565	33.05	0.40	0.70	1.76	5.75	0.43	0.43	-0.16	0.55	1.31	2.49	0.70	1.06
13	49586	8033	19195	38.07	0.41	0.72	1.80	6.17	0.42	0.44	-0.16	0.57	1.31	2.58	0.72	1.08
14	49496	8589	19502	33.19	0.39	0.70	1.76	5.76	0.44	0.43	-0.16	0.56	1.31	2.54	0.70	1.06
15	52225	8699	20358	36.02	0.40	0.71	1.79	6.00	0.43	0.44	-0.16	0.56	1.31	2.57	0.71	1.07

No	Nir	Red	Green	RNDVI	MPRI	NDVI	EVI2	RVI	RGRI	GNDVI	NDGRI	NDVSI	TNDVI	GRVI	OSAVI	SAVI
							Class Name: Ripening Rice									
1	38013	12504	17381	9.24	0.16	0.50	1.26	3.04	0.72	0.37	-0.09	0.44	1.23	2.19	0.50	0.76
2	30973	10185	15877	9.25	0.22	0.51	1.26	3.04	0.64	0.32	-0.12	0.41	1.23	1.95	0.51	0.76
3	33809	10701	15922	9.98	0.20	0.52	1.30	3.16	0.67	0.36	-0.10	0.44	1.23	2.12	0.52	0.78
4	35486	11073	15650	10.27	0.17	0.52	1.31	3.20	0.71	0.39	-0.09	0.45	1.23	2.27	0.52	0.79
5	36648	11120	16612	10.86	0.20	0.53	1.34	3.30	0.67	0.38	-0.10	0.45	1.24	2.21	0.53	0.80
6	48431	14598	26086	11.00	0.28	0.54	1.34	3.32	0.56	0.30	-0.15	0.41	1.24	1.86	0.54	0.81
7	36482	10477	16334	12.12	0.22	0.55	1.38	3.48	0.64	0.38	-0.11	0.46	1.25	2.23	0.55	0.83
8	48736	13773	24439	12.52	0.28	0.56	1.40	3.54	0.56	0.33	-0.15	0.44	1.25	1.99	0.56	0.84
9	36836	10248	16917	12.92	0.25	0.56	1.41	3.59	0.61	0.37	-0.12	0.46	1.25	2.18	0.56	0.85
10	53413	14557	25479	13.46	0.27	0.57	1.43	3.67	0.57	0.35	-0.14	0.45	1.25	2.10	0.57	0.86
11	53229	13945	26154	14.57	0.30	0.58	1.46	3.82	0.53	0.34	-0.15	0.45	1.26	2.04	0.58	0.88
12	53247	13627	26282	15.26	0.32	0.59	1.48	3.91	0.52	0.34	-0.16	0.45	1.26	2.03	0.59	0.89
13	39744	9975	17664	15.87	0.28	0.60	1.50	3.98	0.56	0.38	-0.13	0.48	1.26	2.25	0.60	0.90
14	52751	12824	24631	16.92	0.32	0.61	1.52	4.11	0.52	0.36	-0.15	0.48	1.27	2.14	0.61	0.91
15	51938	12161	23995	18.23	0.33	0.62	1.55	4.27	0.51	0.37	-0.16	0.48	1.27	2.16	0.62	0.93

No	Nir	Red	Green	RNDVI	MPRI	NDVI	EVI2	RVI	RGRI	GNDVI	NDGRI	NDVSI	TNDVI	GRVI	OSAVI	SAVI
							Class Name: Trees									
1	34045	4152	22914	67.10	0.69	0.78	1.96	8.20	0.18	0.20	-0.33	0.43	1.34	1.49	0.78	1.17
2	53092	5930	27205	80.04	0.64	0.80	2.00	8.95	0.22	0.32	-0.26	0.52	1.34	1.95	0.80	1.20
3	53047	5834	26291	82.55	0.64	0.80	2.00	9.09	0.22	0.34	-0.26	0.54	1.34	2.02	0.80	1.20
4	46723	5112	22268	83.39	0.63	0.80	2.01	9.14	0.23	0.35	-0.25	0.55	1.34	2.10	0.80	1.20
5	46629	5047	22053	85.20	0.63	0.80	2.01	9.24	0.23	0.36	-0.25	0.55	1.34	2.11	0.80	1.21
6	53101	4114	24179	166.08	0.71	0.86	2.14	12.91	0.17	0.37	-0.26	0.58	1.36	2.20	0.86	1.28
7	47606	3686	16720	166.22	0.64	0.86	2.14	12.92	0.22	0.48	-0.20	0.65	1.36	2.85	0.86	1.28
8	51556	3991	22365	166.34	0.70	0.86	2.14	12.92	0.18	0.39	-0.25	0.59	1.36	2.31	0.86	1.28
9	50604	3915	22378	166.52	0.70	0.86	2.14	12.93	0.17	0.39	-0.25	0.59	1.36	2.26	0.86	1.28
10	53321	4121	21365	166.89	0.68	0.86	2.14	12.94	0.19	0.43	-0.23	0.61	1.36	2.50	0.86	1.28
11	53074	2473	21515	456.63	0.79	0.91	2.28	21.46	0.11	0.42	-0.26	0.63	1.38	2.47	0.91	1.37
12	49682	2253	23089	481.55	0.82	0.91	2.28	22.05	0.10	0.37	-0.29	0.59	1.38	2.15	0.91	1.37
13	53128	2359	20598	502.42	0.79	0.91	2.29	22.52	0.11	0.44	-0.25	0.64	1.38	2.58	0.91	1.37
14	53101	2166	20612	594.29	0.81	0.92	2.30	24.52	0.11	0.44	-0.25	0.65	1.39	2.58	0.92	1.38
15	53720	2186	20632	597.20	0.81	0.92	2.30	24.57	0.11	0.45	-0.25	0.65	1.39	2.60	0.92	1.38

Appendix 3   Training Data Statistics

Input	Class	Min	Max	Average	STDEV	Input	Class	Min	Max	Average	STDEV
Red	1	17826	35828	26900.7	3713.73	RGRI	1	1.4315	3.397	2.132546	0.22992
	2	10291	15037	12619.4	746.574		2	0.7226	1.065	0.890231	6.37E-02
	3	4735	10163	6858.04	957.841		3	0.2444	0.597	0.376727	7.69E-02
	4	5769	9535	7568.79	702.051		4	0.3518	0.531	0.430319	3.23E-02
	5	8401	16306	11567.6	1763.2		5	0.4456	0.897	0.589326	5.71E-02
	6	2112	6769	4238.64	803.101		6	0.0976	0.269	0.186736	2.98E-02
Green	1	7039	16877	12661.1	1508.75	GNDVI	1	-0.2803	0.207	-0.01295	0.1121
	2	13023	15401	14192.9	417.692		2	0.2906	0.408	0.341364	1.95E-02
	3	13781	22773	18455.6	1609.92		3	0.3498	0.534	0.452961	3.18E-02
	4	14861	21670	17628	1539.81		4	0.3543	0.504	0.446594	2.17E-02
	5	15184	26927	19905.4	4136.93		5	0.265	0.468	0.365114	3.16E-02
	6	15850	27748	22705.4	2281.77		6	0.107	0.513	0.381661	5.61E-02
NIR	1	4289	18386	12515.4	2470.07	NDRGI	1	0.1911	1.295	0.581332	0.16725
	2	25269	34495	28941.7	1525.47		2	-0.0942	0.021	-3.62E-02	2.11E-02
	3	34659	54139	49206.8	5215.86		3	-0.2203	-0.108	-0.17	2.01E-02
	4	35031	53794	46105.5	3919.84		4	-0.2087	-0.121	-0.15778	1.28E-02
	5	30100	53989	42560.7	7193.57		5	-0.2011	-0.029	-0.13089	2.26E-02
	6	26618	55363	50832.1	4218.39		6	-0.369	-0.185	-0.25146	2.49E-02
RNDVI	1	0.0479	0.90301	0.24809	0.13227	NDVSI	1	-0.5153	0.077	-0.2277	0.12727
	2	3.4728	8.35248	5.33527	0.88641		2	0.2995	0.444	0.366206	2.37E-02
	3	16.188	118.429	56.6796	20.8294		3	0.4776	0.652	0.588103	3.76E-02
	4	27.382	52.8702	37.5056	5.42016		4	0.5064	0.618	0.570436	1.66E-02
	5	7.7423	19.8791	13.631	2.15652		5	0.3846	0.535	0.460613	2.35E-02
	6	39.39	598.142	160.75	70.1702		6	0.3487	0.683	0.579826	4.46E-02
MPRI	1	-0.545	-0.1775	-0.3582	4.53E-02	TNDVI	1	0.5994	0.987	0.793785	8.10E-02
	2	-0.031	0.16101	5.93E-02	3.55E-02		2	1.1409	1.219	1.179874	1.49E-02
	3	0.2522	0.6072	0.45705	0.07761		3	1.2657	1.353	1.323286	2.07E-02
	4	0.3061	0.47949	0.399	3.14E-02		4	1.2958	1.326	1.310588	6.59E-03
	5	0.0542	0.38355	0.26001	0.04508		5	1.213	1.278	1.253368	0.01084
	6	0.5766	0.82219	0.68636	4.25E-02		6	1.3135	1.386	1.358456	1.08E-02
NDVI	1	-0.641	-0.0255	-0.3633	0.12606	GRVI	1	0.5621	1.523	0.997843	0.21232
	2	0.3016	0.48592	0.39232	0.03503		2	1.8191	2.38	2.039262	9.08E-02
	3	0.6019	0.83186	0.75151	5.43E-02		3	2.076	3.289	2.668163	0.20912
	4	0.6792	0.75831	0.71768	1.73E-02		4	2.0974	3.036	2.619394	0.13816
	5	0.4713	0.63368	0.57105	2.71E-02		5	1.721	2.761	2.158027	0.15821
	6	0.7253	0.92187	0.84552	2.94E-02		6	1.2396	3.111	2.259959	0.28444
EVI2	1	-1.602	-0.0637	-0.9084	0.31514	OSAVI	1	-0.6407	-0.025	-0.36335	0.12605
	2	0.754	1.2148	0.98081	8.76E-02		2	0.3016	0.486	0.392322	3.50E-02
	3	1.5048	2.07966	1.87878	0.13581		3	0.6019	0.832	0.751511	5.43E-02
	4	1.698	1.89578	1.79421	4.32E-02		4	0.6792	0.758	0.717681	1.73E-02
	5	1.1782	1.5842	1.42762	6.79E-02		5	0.4713	0.634	0.571046	2.71E-02
	6	1.8133	2.30468	2.1138	7.35E-02		6	0.7253	0.922	0.845518	2.94E-02
RVI	1	0.219	0.95032	0.47942	0.13525	SAVI	1	-0.961	-0.038	-0.54501	0.18908
	2	1.8637	2.89045	2.30217	0.19074		2	0.4524	0.729	0.588478	5.25E-02
	3	4.0243	10.895	7.37769	1.52349		3	0.9029	1.248	1.12726	8.15E-02
	4	5.2344	7.27513	6.111	0.4391		4	1.0188	1.137	1.076515	2.59E-02
	5	2.7828	4.45969	3.681	0.29302		5	0.7069	0.951	0.856564	4.07E-02
	6	6.2808	24.599	12.429	2.62161		6	1.0879	1.383	1.268269	4.41E-02

* Class 1 : Fallow/Non Vegetation   Class 3 : Vegetative Rice   Class 5 : Ripening Rice

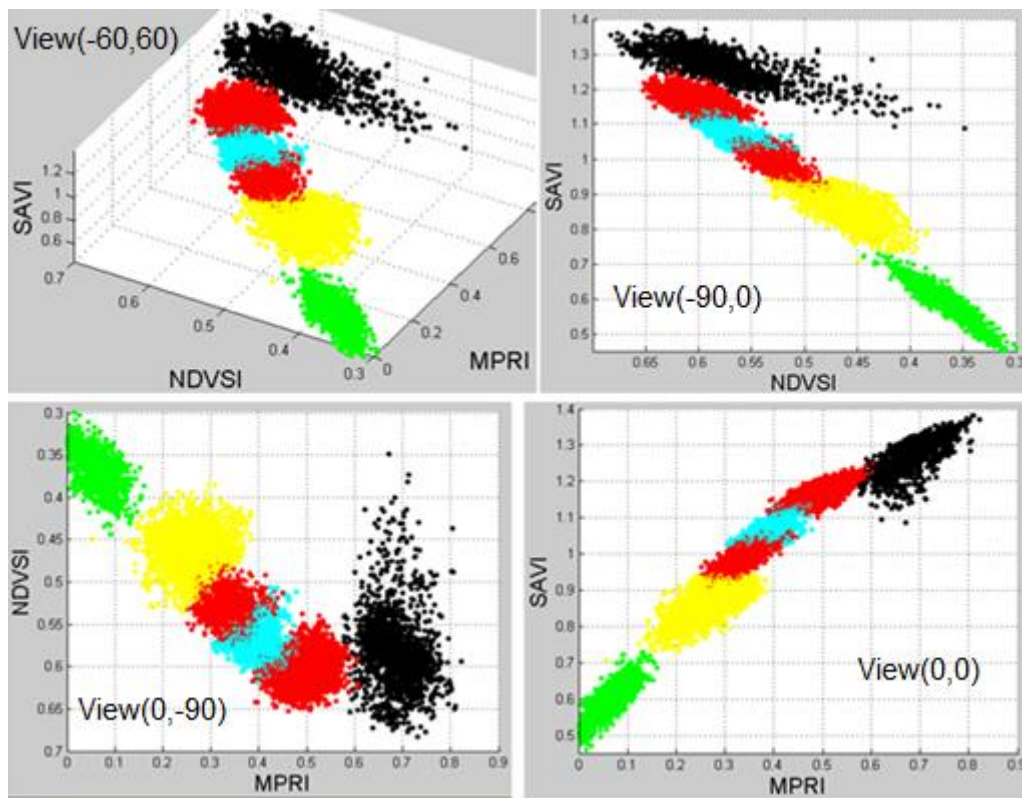Class 2 : New Rice Planting   Class 4 : Reproductive Rice   Class 6 : Trees

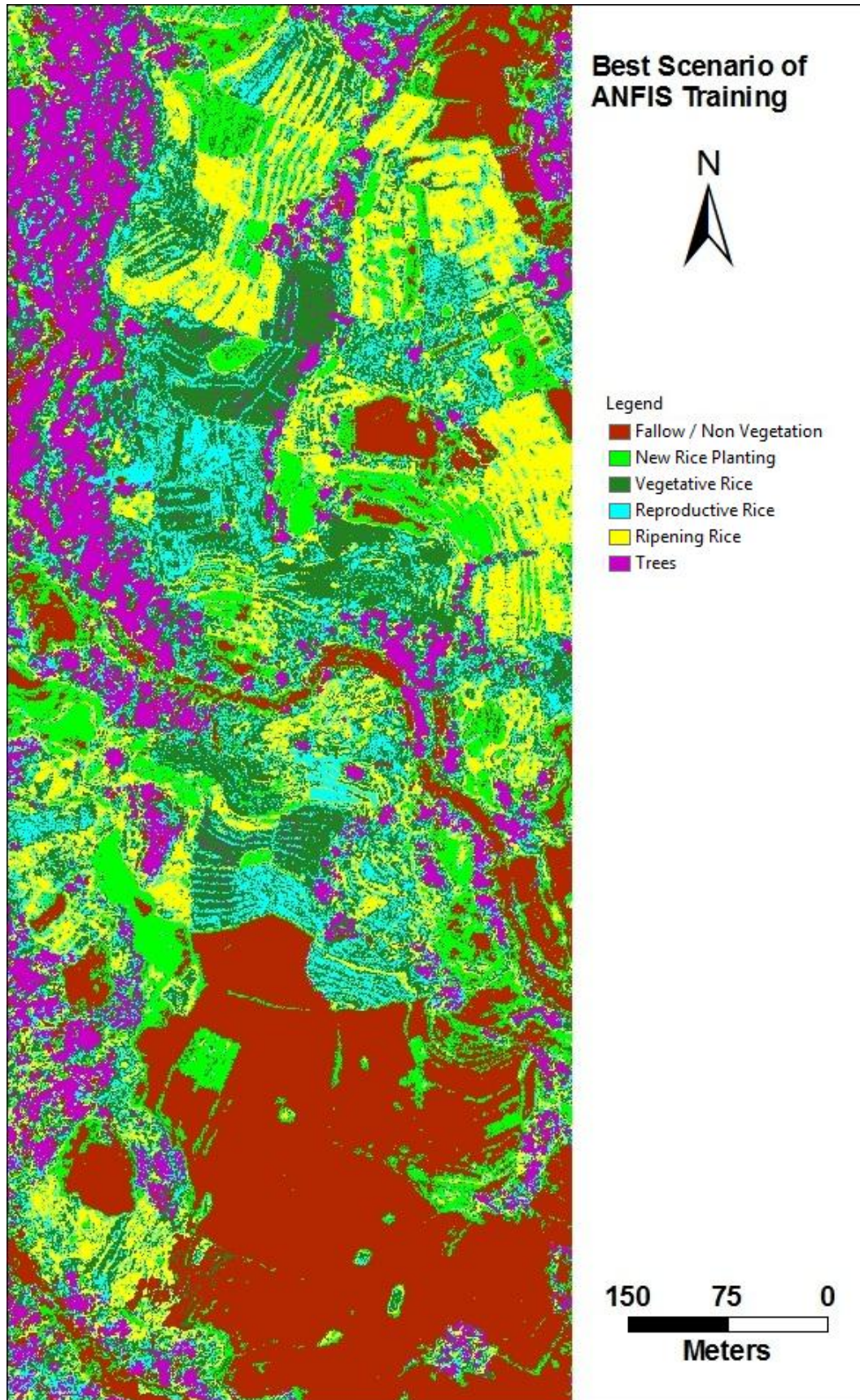Appendix 4   Normal Distribution Curve

2

50
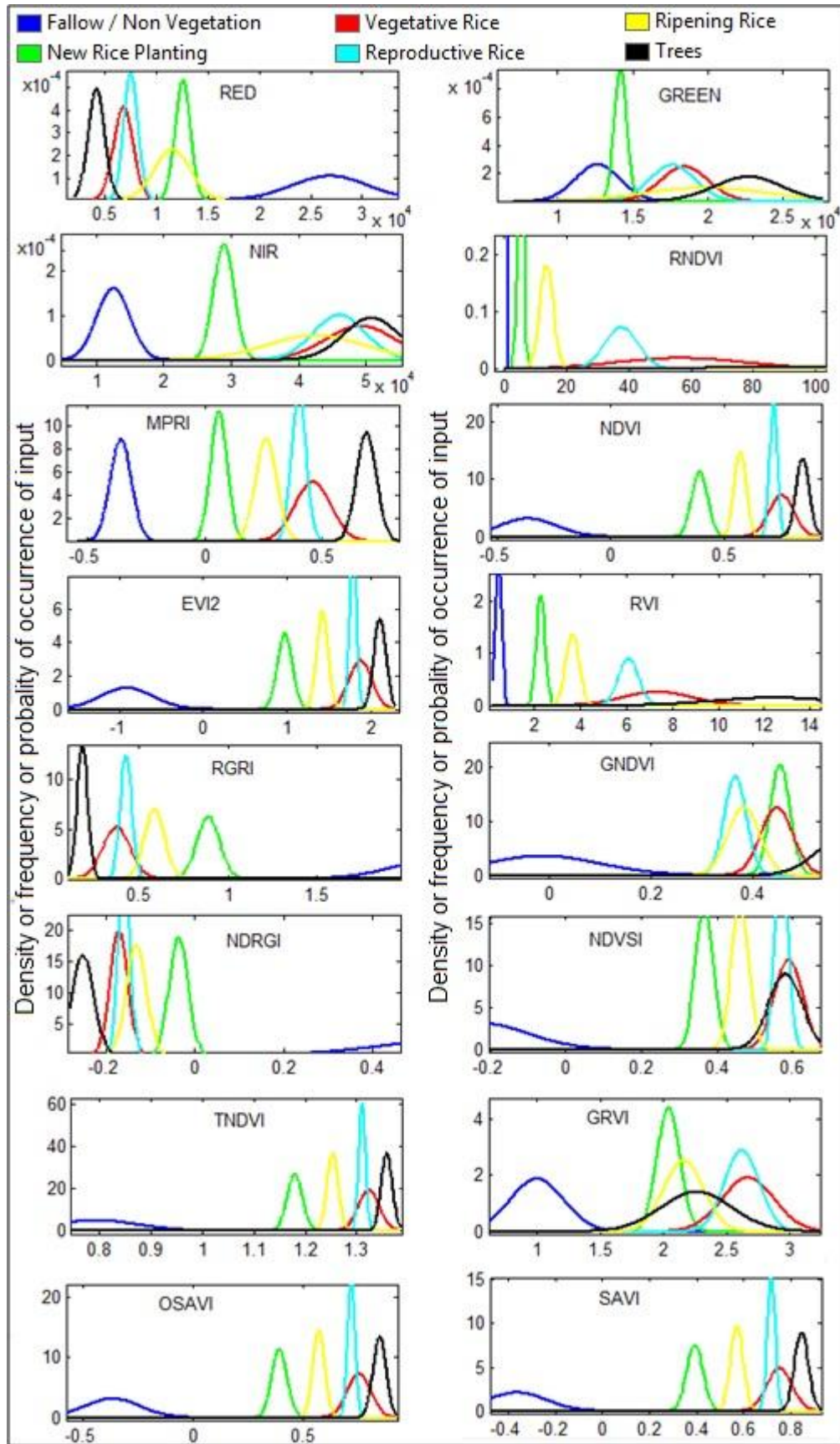
Appendix 5   3-D Scatter Graph of Training Data
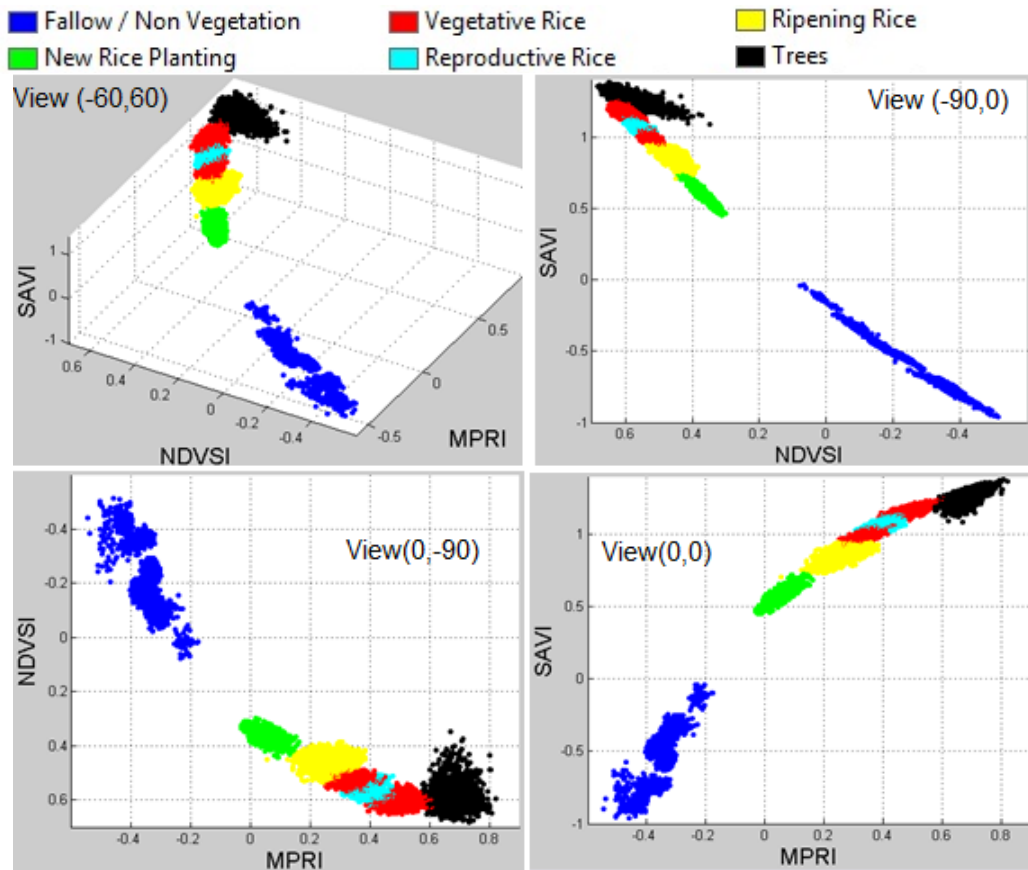
Zoom of the graph

Appendix 6   Mapping Using Best Scenario of ANFIS Training

Appendix 7   Sample of Calculation

1. Convert Original image to image ratio using formula in Table 2-1.
2. Calculate membership degree using trapezoid membership function, where parameter membership function is described in Table 4-6.

$$\text{trapezoid}(x; a, b, c, d) = \max\left(\min\left(\frac{x-a}{b-a}, 1, \frac{d-x}{d-c}\right), 0\right)$$

Calculation of step 1 and 2 is describes in table below.

Data Set	Original			Rationing			μ MPRI			μ NDVSI			μ SAVI		
	Nir	Red	Green	MPRI	NDVSI	SAVI	Low	Mdium	High	Low	Mdium	High	Low	Mdium	High
1	44425	7114	16626	0.40	0.58	1.09	0.00	1.00	0.32	0.00	0.00	0.88	0.00	0.00	1.00
2	33809	10701	15922	0.20	0.44	0.78	0.00	1.00	0.00	0.00	1.00	0.47	0.00	0.56	0.24
3	34045	4152	22914	0.69	0.43	1.17	0.00	0.00	0.97	0.00	1.00	0.46	0.00	0.00	1.00
4	5990	23908	7039	-0.55	-0.44	-0.90	1.00	0.00	0.00	1.00	0.00	0.00	1.00	0.00	0.00
5	29923	12241	14444	0.08	0.38	0.63	0.00	1.00	0.00	0.00	1.00	0.32	0.00	0.86	0.00
6	44409	9327	16816	0.29	0.55	0.98	0.00	1.00	0.07	0.00	0.00	0.78	0.00	0.17	0.82

3. Calculate premise output each data set. Multiply each combination membership degree. Calculation of step 3 is describes in table below.

i (Rule)	wi	μ MPRI. μ NDVSI.μ SAVI.			Premise output each data set					
					1	2	3	4	5	6
1	w1 =	MPRI Low	.NDVSI Low	.SAVI Low =	0.00	0.00	0.00	1.00	0.00	0.00
2	w2 =	MPRI Low	.NDVSI Low	.SAVI medium =	0.00	0.00	0.00	0.00	0.00	0.00
3	w3 =	MPRI Low	.NDVSI Low	.SAVI High =	0.00	0.00	0.00	0.00	0.00	0.00
4	w4 =	MPRI Low	.NDVSI medium	.SAVI Low =	0.00	0.00	0.00	0.00	0.00	0.00
5	w5 =	MPRI Low	.NDVSI medium	.SAVI medium =	0.00	0.00	0.00	0.00	0.00	0.00
6	w6 =	MPRI Low	.NDVSI medium	.SAVI High =	0.00	0.00	0.00	0.00	0.00	0.00
7	w7 =	MPRI Low	.NDVSI High	.SAVI Low =	0.00	0.00	0.00	0.00	0.00	0.00
8	w8 =	MPRI Low	.NDVSI High	.SAVI medium =	0.00	0.00	0.00	0.00	0.00	0.00
9	w9 =	MPRI Low	.NDVSI High	.SAVI High =	0.00	0.00	0.00	0.00	0.00	0.00
10	w10 =	MPRI medium	.NDVSI Low	.SAVI Low =	0.00	0.00	0.00	0.00	0.00	0.00
11	w11 =	MPRI medium	.NDVSI Low	.SAVI medium =	0.00	0.00	0.00	0.00	0.00	0.00
12	w12 =	MPRI medium	.NDVSI Low	.SAVI High =	0.00	0.00	0.00	0.00	0.00	0.00
13	w13 =	MPRI medium	.NDVSI medium	.SAVI Low =	0.00	0.00	0.00	0.00	0.00	0.00
14	w14 =	MPRI medium	.NDVSI medium	.SAVI medium =	0.00	0.56	0.00	0.00	0.86	0.00
15	w15 =	MPRI medium	.NDVSI medium	.SAVI High =	0.00	0.24	0.00	0.00	0.00	0.00
16	w16 =	MPRI medium	.NDVSI High	.SAVI Low =	0.00	0.00	0.00	0.00	0.00	0.00
17	w17 =	MPRI medium	.NDVSI High	.SAVI medium =	0.00	0.26	0.00	0.00	0.27	0.13
18	w18 =	MPRI medium	.NDVSI High	.SAVI High =	0.88	0.11	0.00	0.00	0.00	0.64
19	w19 =	MPRI High	.NDVSI Low	.SAVI Low =	0.00	0.00	0.00	0.00	0.00	0.00
20	w20 =	MPRI High	.NDVSI Low	.SAVI medium =	0.00	0.00	0.00	0.00	0.00	0.00
21	w21 =	MPRI High	.NDVSI Low	.SAVI High =	0.00	0.00	0.00	0.00	0.00	0.00
22	w22 =	MPRI High	.NDVSI medium	.SAVI Low =	0.00	0.00	0.00	0.00	0.00	0.00
23	w23 =	MPRI High	.NDVSI medium	.SAVI medium =	0.00	0.00	0.00	0.00	0.00	0.00
24	w24 =	MPRI High	.NDVSI medium	.SAVI High =	0.00	0.00	0.97	0.00	0.00	0.00
25	w25 =	MPRI High	.NDVSI High	.SAVI Low =	0.00	0.00	0.00	0.00	0.00	0.00
26	w26 =	MPRI High	.NDVSI High	.SAVI medium =	0.00	0.00	0.00	0.00	0.00	0.01
27	w27 =	MPRI High	.NDVSI High	.SAVI High =	0.28	0.00	0.44	0.00	0.00	0.05
		∑ wi			1.16	1.18	1.42	1.00	1.13	0.82

Appendix 7   (Continued)

4. Calculate consequent output each data set using linier equation in table 4-7.
5. Calculate rule output each data set using multiply premise and consequent output.

Calculation of step 4 and 5 is describes in table below.

i (Rule)	fi	Consequent output each data set					
		1	2	3	4	5	6
1	f1 =	0.82	0.85	0.72	1.00	0.87	0.84
2	f2 =	33.45	25.81	43.64	-4.96	21.55	29.48
3	f3 =	0.00	0.00	0.00	0.00	0.00	0.00
4	f4 =	-2.04	-1.87	-5.99	0.05	-1.31	-1.89
5	f5 =	-13.53	-11.97	-31.17	-4.32	-9.30	-12.14
6	f6 =	0.00	0.00	0.00	0.00	0.00	0.00
7	f7 =	0.00	0.00	0.00	0.00	0.00	0.00
8	f8 =	0.00	0.00	0.00	0.00	0.00	0.00
9	f9 =	0.00	0.00	0.00	0.00	0.00	0.00
10	f10 =	-3.16	-3.27	0.16	0.07	-3.57	-3.69
11	f11 =	15.20	6.26	33.41	-20.81	0.86	9.50
12	f12 =	0.00	0.00	0.00	0.00	0.00	0.00
13	f13 =	-8.06	-5.84	-12.69	5.13	-4.34	-7.01
14	f14 =	-1.91	0.63	-0.78	10.04	1.51	-0.73
15	f15 =	8.43	11.20	-57.89	97.26	22.28	6.15
16	f16 =	0.00	0.00	0.00	0.00	0.00	0.00
17	f17 =	-16.78	4.50	58.24	53.47	3.51	-7.17
18	f18 =	3.30	12.64	-5.63	73.69	18.23	5.95
19	f19 =	0.00	0.00	0.00	0.00	0.00	0.00
20	f20 =	0.00	0.00	0.00	0.00	0.00	0.00
21	f21 =	0.00	0.00	0.00	0.00	0.00	0.00
22	f22 =	0.00	0.00	0.00	0.00	0.00	0.00
23	f23 =	186.06	27.68	252.13	-828.28	-51.53	129.37
24	f24 =	3.35	3.45	5.95	12.49	3.48	2.53
25	f25 =	0.00	0.00	0.00	0.00	0.00	0.00
26	f26 =	-46.81	-94.44	-69.30	-365.84	-113.96	-60.74
27	f27 =	5.63	6.65	6.12	15.29	7.16	5.68

fi.wi	Rule output each data set					
	1	2	3	4	5	6
f1.w1=	0.00	0.00	0.00	1.00	0.00	0.00
f2.w2=	0.00	0.00	0.00	0.00	0.00	0.00
f3.w3=	0.00	0.00	0.00	0.00	0.00	0.00
f4.w4=	0.00	0.00	0.00	0.00	0.00	0.00
f5.w5=	0.00	0.00	0.00	0.00	0.00	0.00
f6.w6=	0.00	0.00	0.00	0.00	0.00	0.00
f7.w7=	0.00	0.00	0.00	0.00	0.00	0.00
f8.w8=	0.00	0.00	0.00	0.00	0.00	0.00
f9.w9=	0.00	0.00	0.00	0.00	0.00	0.00
f10.w10=	0.00	0.00	0.00	0.00	0.00	0.00
f11.w11=	0.00	0.00	0.00	0.00	0.00	0.00
f12.w12=	0.00	0.00	0.00	0.00	0.00	0.00
f13.w13=	0.00	0.00	0.00	0.00	0.00	0.00
f14.w14=	0.00	0.35	0.00	0.00	1.29	0.00
f15.w15=	0.00	2.72	0.00	0.00	0.00	0.00
f16.w16=	0.00	0.00	0.00	0.00	0.00	0.00
f17.w17=	0.00	1.18	0.00	0.00	0.96	-0.94
f18.w18=	2.89	1.43	0.00	0.00	0.00	3.79
f19.w19=	0.00	0.00	0.00	0.00	0.00	0.00
f20.w20=	0.00	0.00	0.00	0.00	0.00	0.00
f21.w21=	0.00	0.00	0.00	0.00	0.00	0.00
f22.w22=	0.00	0.00	0.00	0.00	0.00	0.00
f23.w23=	0.00	0.00	0.00	0.00	0.00	0.00
f24.w24=	0.00	0.00	5.80	0.00	0.00	0.00
f25.w25=	0.00	0.00	0.00	0.00	0.00	0.00
f26.w26=	0.00	0.00	0.00	0.00	0.00	-0.57
f27.w27=	1.60	0.00	2.71	0.00	0.00	0.26
∑ fi.wi	4.49	5.69	8.51	1.00	2.25	2.54

6. Calculate final output each data set using divide sigma rule output with sigma premise output. Define class output using target and range value in table 4-8. Calculation of step 6 is describes in table below.

No data Set	∑ fi.wi	∑ wi	∑ fi.wi/∑ wi	Range Value	Target Value	Class
1	4.49	1.16	3.87	3.5 - 4.5	4	Reproductive Rice
2	5.69	1.18	4.81	4.5 - 5.5	5	Ripening Rice
3	8.51	1.42	6.00	> 5.5	6	Trees
4	1.00	1.00	1.00	< 1.5	1	Fallow / Non Vegetation
5	2.25	1.13	1.99	1.5 - 2.5	2	New Rice Planting
6	2.54	0.82	3.08	2.5 - 3.5	3	Vegetative Rice

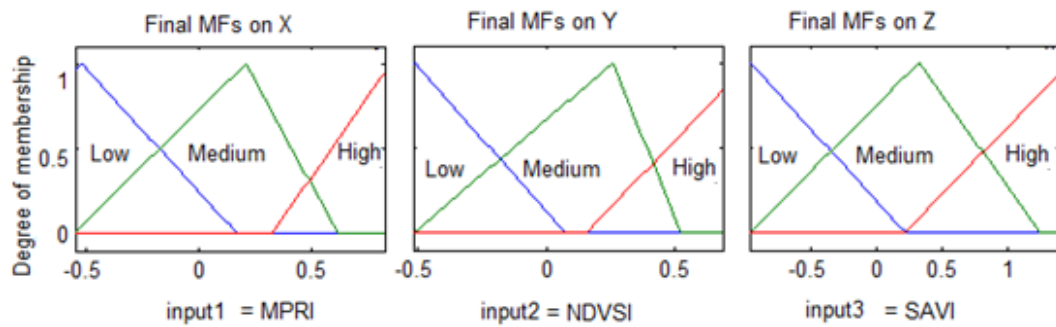Appendix 8 Map of Rice Plant Growth Stage

Appendix 9   Final Membership Functions of Scenarios 21 to 24

21. Triangle Membership Function

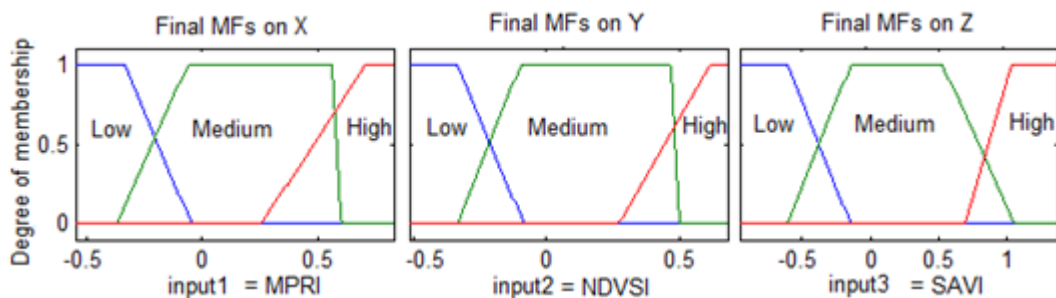$$\text{triangle}(x; a, b, c) = \max\left(\min\left(\frac{x-a}{b-a}, \frac{c-x}{c-b}\right), 0\right)$$

Variable Fuzzy	Membership function								
	Low			Medium			High		
	a	b	c	a	b	c	a	b	c
MPRI (X)	-1.23	-0.52	0.17	-0.55	0.21	0.62	0.32	0.85	1.51
NDVSI (Y)	-1.11	-0.51	0.08	-0.52	0.26	0.52	0.15	0.79	1.28
SAVI (Z)	-2.13	-0.96	0.23	-0.96	0.32	1.25	0.21	1.47	2.55

22. Trapezoid Membership Function

$$\text{trapezoid}(x; a, b, c, d) = \max\left(\min\left(\frac{x-a}{b-a}, 1, \frac{d-x}{d-c}\right), 0\right)$$

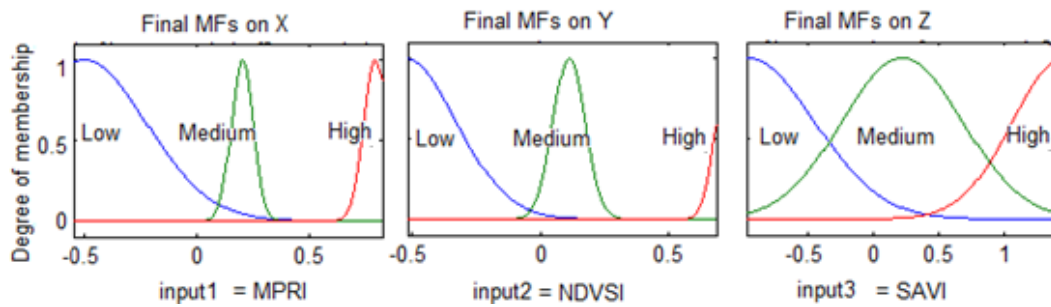| Variable Fuzzy	Membership function											
	Low				Medium				High			
	a	b	c	d	a	b	c	d	a	b	c	d
MPRI (X)	-1.024	-0.750	-0.333	-0.046	-0.367	-0.060	0.557	0.596	0.254	0.705	1.027	1.301
NDVSI (Y)	-0.935	-0.695	-0.334	-0.083	-0.334	-0.095	0.469	0.502	0.272	0.622	0.863	1.102
SAVI (Z)	-1.781	-1.313	-0.608	-0.142	-0.609	-0.139	0.532	1.065	0.694	1.044	1.734	2.203

Appendix 9   (Continued)

23. Gaussian Membership Function

$$\text{gaussian}(x; c, \sigma) = e^{-\frac{1}{2}\left(\frac{x-c}{\sigma}\right)^2}.$$

Variable Fuzzy	Membership function					
	Low		Medium		High	
	δ	c	δ	c	δ	c
MPRI (X)	0.28	-0.50	0.05	0.20	0.05	0.79
NDVSI (Y)	0.20	-0.53	0.06	0.11	0.05	0.73
SAVI (Z)	0.51	-0.95	0.46	0.22	0.39	1.45

24. General Bell Membership Function

$$\text{bell}(x; a, b, c) = \frac{1}{1 + \left|\frac{x-c}{a}\right|^{2b}},$$

Variable Fuzzy	Membership function								
	Low			Medium			High		
	a	b	c	a	b	c	a	b	c
MPRI (X)	0.39	2.02	-0.46	0.06	2.04	0.23	0.03	2.11	0.67
NDVSI (Y)	0.41	1.98	-0.48	0.11	2.04	0.25	0.05	2.03	0.62
SAVI (Z)	0.75	1.94	-0.90	0.44	2.07	0.26	0.31	2.04	1.50